ALMA MATER STUDIORUM
UNIVERSITA' DI BOLOGNA

FACOLTA' DI SCIENZE MATEMATICHE FISICHE E NATURALI

Corso di laurea magistrale in BIOLOGIA MARINA

"Ecological modelling of the phytoplankton dynamics in the northern Gulf of Aqaba (Red Sea)"

Tesi di laurea in Evoluzione ed Adattamenti degli Invertebrati Marini

Relatore
Dr. Stefano Goffredo
(Università di Bologna)

Presentata da
Leonardo Laiolo

Correlatori
Dr. Alberto Barausse (Università di Padova)
Prof. Luca Palmeri (Università di Padova)
Dr. David Iluz (Bar-Ilan University, Israele)
Prof. Zvy Dubinsky (Bar-Ilan University, Israele)

I sessione
Anno Accademico 2011-2012

"The sciences do not try to explain, they hardly even try to interpret, they mainly make models. By a model is meant a mathematical construct which, with the addition of certain verbal interpretations describes observed phenomena. The justification of such a mathematical construct is solely and precisely that it is expected to work"

John von Neumann

CONTENTS

ABSTRACT

The Gulf of Aqaba represents a small scale, easy to access, regional analogue of larger oceanic oligotrophic systems. In this Gulf, the seasonal cycles of stratification and vertical mixing drive the annual phytoplankton dynamics and patterns. In summer and fall, when nutrient concentrations are very low, *Prochlorococcus* and *Synechococcus* are more abundant in the surface waters. At that time these two populations are exposed to phosphate limitation. During winter mixing, when nutrient concentrations are higher, *Chlorophyceae* and *Cryptophyceae* become dominant but are scarce or absent during summer.

In this study it was tried to develop a simulation model based on historical data to predict the phytoplankton dynamics in the northern Gulf of Aqaba. The purpose is to understand what forces operate, and how, to control the phytoplankton dynamics in the Gulf.

For the models data sampled in two different sampling station (*Fish Farm Station* and *Station A*) were used, concomitant with data of chemical, biological and physical factors, from 14th January 2007 to 28th December 2009. The *Fish Farm Station* point was near a Fish Farm that was operational until 17th June 2008, the complete closure date of the Fish Farm, about halfway through the total sampling period. The *Station A* sampling point is about 13 km away from the *Fish Farm Station*. To build the model, the MATLAB software package was used (version 7.6.0.324 R2008a), in particular a tool named *Simulink.*

The *Fish Farm Station* models shows that the Fish Farm activity has altered the nutrient concentrations and as a consequence affected the normal phytoplankton dynamics. Despite the considerable distance between the two sampling stations, there might be some influence from the Fish Farm activities also on the *Station A* ecosystem. The models of this sampling station show that the Fish Farm impact appears to be much lower than in the *Fish Farm Station*, because the phytoplankton dynamics at Station A appear to be driven mainly by the seasonal mixing cycle.

INTRODUCTION

DESCRIPTION OF THE ECOSYSTEM

The Gulf of Aqaba is one of two large gulfs in the Red Sea, located to the east of the Sinai Peninsula and west of the Arabian mainland, separated from the Red Sea by the 252 m deep sill at the Straits of Tiran (Fig. 1). This Gulf is 170 km long and 14-24 km wide, with an average depth of 800 meters and a maximum of 1830 meters. For these reasons the Gulf of Aqaba represents a small scale, easy to access, regional analogue of larger oceanic oligotrophic systems (Chen et al. 2008).

Fig. 1: *Gulf of Aqaba with the position of Eilat (Israel) and Aqaba (Jordan)*

In the Gulf of Aqaba the climate is extremely arid, the yearly precipitation at the northern gulf averages only 30 mm, and hot, with summer air temperature reaching up to 45°C, with prevailing northerly winds. Excess evaporation over this minimal precipitation is in the range of 2000 mmy^{-1} (Monismith et al. 2006). No rivers flow into the gulf, and fresh water, other than rain, reaches it only occasionally during rare winter floods.

The two largest cities in this area are Eilat (Israel) and Aqaba (Jordan), these cities rise in front of a coral reef that supports a complex and fragile ecosystem. Southern Eilat, where the nature reserve "Coral Beach" was set up in 1974, encompasses the northernmost coral reef in the world.

The coral reef stretches over 1200 metres along the west coast of the Bay of Eilat and inspite of its marginal position as a coral reef, it has more than 1000 different species of corals and accommodates a wide biodiversity of fish species and invertebrates, including several endemic species. The coral reef, in front of the city of Eilat and Aqaba, supports a thriving economy based primarily on tourism. Environmental factors might threaten this important source of revenue; in particular some studies show a worsening of sea-water quality due to human activity and industrial pollution in the coastal zones surrounding the Gulf: metallurgical industries, hotels and resorts, port activities and fish farming (Chen Y et al. 2008, Lazar B et al. 2008, Loya Y et al. 2003, Loya Y et al. 2004). Global climate change may also be a contributory factor: the dust deposit in the Gulf due to desertification processes, water warming and acidification caused by an anthropogenic increase in atmospheric greenhouse gases, and increase in UV radiation due to ozone depletion (Lazar B et al. 2008, Chen Y et al. 2007, Chen Y et al. 2008). A combination of these factors may play a role in deteriorating reef conditions.

This area is dominated by mineral dust deposition and surrounded by deserts; anthropogenic air emissions may make a significant contribution to the level of various trace of elements such as Cu, Cd, Ni, Zn (Chen et al. 2008). Relative isolation from the main Red Sea and the Indian Ocean, intense solar radiation for most of the year, low plankton biomass, and low POM (Particulate Organic Matter) characterize the Gulf of Aqaba. The low levels of nitrogen and phosphate nutrients are the main limiting factors in the Gulf of Aqaba (Al-Qutob et al. 2002, Labiosa et al. 2003). In recent years it has been seen that the atmospheric inputs of other nutrients gradually increase the likelihood of P limitation in the Gulf (Chen et al. 2007). As a result of these studies it has been recognized that P limitation in the ocean may be more prevalent than previously estimated, and that the efficiency of P uptake among individual groups of phytoplankton may, in fact, control the phytoplankton species composition observed in a given community. Furthermore, it has been suggested that a transition from N limitation to P limitation has taken place over the last two decades in the

North Pacific Subtropical Gyre, and that this favours the growth of prokaryotic picophytoplankton, such as *Prochlorococcus* and *Synechococcus*, which have a large surface area to volume ratio and take up nutrients more efficiently than larger phytoplankton (Karl et al. 2001).

SEASONAL CYCLES OF STRATIFICATION AND MIXING

The Gulf of Aqaba has similar seasonal cycles of stratification and mixing to other subtropical oligotrophic seas. Small perturbations such as transient cooling (that induces convection) and wind events (that drive upwelling) can at times inject deep water to the surface euphotic layer, making nutrients available for phytoplankton growth (Labiosa et al. 2003). When the mixing layer exceeds a critical depth phytoplankton bloom cannot develop (Sverdrup 1953).

The water column of the northern Gulf of Aqaba is stratified during summer, and, under normal conditions, surface water nutrient levels are near the limits of detection (Levanon-Spanier et al. 1979, Mackey et al. 2007). During the summer months atmospheric dry deposition is a significant source of nutrients to the euphotic zone, supporting transient phytoplankton blooms (Chen et al.2007, Paytan et al. 2009). Beginning in the fall, cooling of surface waters initiates a convective mixing, and a deeply mixed (300 meters or more) water body is observed by winter (Wolf-Vetch et al. 1992). During winter and early spring the convective component of entrainment is strong enough to mix the surface waters below the critical depth as well as bring large quantities of the nutrients to the surface (Labiosa et al. 2003). The water column begins to re-stratify in the spring as surface waters warm, trapping nutrients and phytoplankton in the euphotic zone along a steep light gradient.

SEASONAL PHYTOPLANKTON DYNAMICS

The nature of the seasonal phytoplankton dynamics may have important implications for trophic interactions within the Gulf of Aqaba (Labiosa et al. 2003). The phytoplankton bloom will have consequences for the food web, consisting of a stronger temporal decoupling between

phytoplankton and zooplankton dynamics (Tagliabue and Arrigo 2003). It has also been shown that the productive coral reefs in the Gulf of Aqaba subsist, for their nutrient supply, to a large degree on allochthonous plankton with nitrogen fluxes from the phytoplankton to the coral reef (Yahel et al. 1998, Richter et al. 2001). In the absence of a significant phytoplankton bloom, phytoplankton may become too scarce to support coral reef production. Therefore, the interannual variability in the intensity and timing of phytoplankton blooms may have serious consequences for the upper trophic levels in the Gulf of Aqaba (Labiosa et al. 2003). Phytoplankton patterns were shown to follow the seasonal hydrological cycle in the Gulf of Aqaba (Iluz et al. 2008).

During winter the Gulf of Aqaba is subjected to benthic injections of nitrogen that maintain the nitrogen phosphorus ratio close to the "Redfield Ratio" (Häse et al. 2006). At this time, eukaryotic algae dominate but their growth rate is limited by light availability with deep mixing (Lindell and Post 1995, Stambler 2005, Al-Najjar et al. 2007). In particular *Chlorophyceae* and *Cryptophyceae* are dominant during winter mixing but scarce or absent during summer (Fig. 2) (Al-Najjar et al. 2007). Water column stratification and the development of the thermocline initiated during spring, entraps nutrients in the high-light surface water resulting in phytoplankton blooms, typically cyanobacteria and diatoms (Lindell and Post 1995, Al-Najjar et al. 2007, Suggett et al. 2009). In particular *Synechococcus* was the main component of phytoplankton during a wind triggered spring bloom of massive proportions (Iluz et al. 2008, Suggett et al. 2009). As spring progresses into summer, the phytoplankton community becomes increasingly dominated by picoeukaryotes and prochlorophytes (Lindell and Post 1995, Al-Najjar et al. 2007, Stambler 2006). Stratification minimizes deep-water injections of nitrogen into near-surface waters, and atmospheric loading of nutrients becomes an important determinant of nutrient availability (Chen et al. 2007).

In summer and fall, when nutrient concentrations are very low, picophytoplankton (cells <2µm) (*Prochlorococcus* and *Synechococcus*) are more abundant in the surface water; in particular *Prochlorococcus* was the

main component of the community during summer stratification (Fig. 2) (Lindell and Post 1995, Post et al. 1996, Mackey et al. 2007). Typically picophytoplankton account for about 37% of phytoplankton cells in winter, whereas they account about 84% of cells in summer and fall, increasing in relative abundance as stratification progresses and nutrients become scarce (Mackey et al. 2007). During summer *Prochlorococcus* and *Synechococcus* populations in the Gulf of Aqaba are exposed to phosphate limitation (Fuller et al. 2005, Mackey et al. 2009).

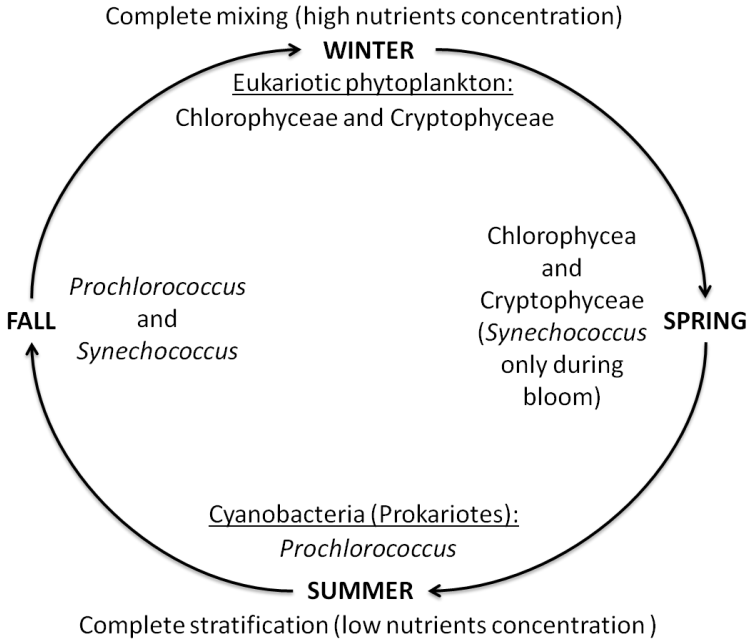

Fig. 2: *The seasonal cycle of stratification and mixing and the phytoplankton constituting the majority of the total chlorophyll a for each season.*

AIM OF THIS STUDY

The aim of this study is to develop a simulation model based on historical data to predict the phytoplankton dynamics in the northern Gulf of Aqaba. The purpose is to understand what forcing functions operate, and how, to control the phytoplankton dynamics in the northern Gulf of Aqaba.

This model might signal deterioration of the waters in front of Aqaba and Eilat due to the Fish Farm activity. This will provide decision-makers with a tool to evaluate the cost/benefit effectiveness of legislative measures under various local developments and global climate change scenarios and to assist in the prevention of potentially detrimental activities. The model

will be useful for future predictions on the environmental conditions in the Gulf of Aqaba and any corrective measures to protect unique high biodiversity of the sensitive ecosystems of the Gulf.

MATERIALS AND METHODS

SAMPLING AND INSTRUMENTS USED

Data sampled in two different sampling station (*Fish Farm Station* and *Station A*) were used in the models. Data were sampled during monthly cruises as part of the project "Protecting the Gulf of Aqaba from Anthropogenic and Natural Stress" supported by the program "The NATO Science for Peace and Security Program (SPS)", aboard the RV "Queen of Sheba". The campaign lasted for the three years from 14th January 2007 to 28th December 2009. A total of 35 *chlorophyll a* measurements and other parameter measurements were sampled for both sampling stations.

Water samples were collected at sampling *Station A* (29°28'N and 34°55'E) and the *Fish Farm Station* (29°32' N and 34°56' E) (Fig 3). The *Fish Farm Station* point was near a Fish Farm that was operational until 17th June 2008, the complete closure date of the Fish Farm, about halfway through the total sampling time. The maximum depth in the *Fish Farm Station* point is 56 meters. The *Station A* sampling point is about 13 km away from the *Fish Farm Station*, and has a 700 m maximum depth and no apparent direct anthropogenic influence.

To collect the parameter measurements and water samples a CTD-Rosette (Sea Bird) equipped with 11 Teflon-coated Niskin bottles (12 L), a CTD (SBE 19-02, SeaBird), Photometer, LICOR (LI-190SA) and a Fluorometer (Sea-Point Sensors Inc.) were used.

The dataset used for building the models contains measurements of: temperature (°C), salinity (ppt), oxygen (micromol/l), pH, alkalinity (meq/kg), NO_3 (micromol/l), SiO_4 (micromol/l), PO_4 (micromol/l), and chlorophyll a (microgr/l). Every measure was performed for both sampling stations. Irradiance data was also available every hour for the three years analyzed.

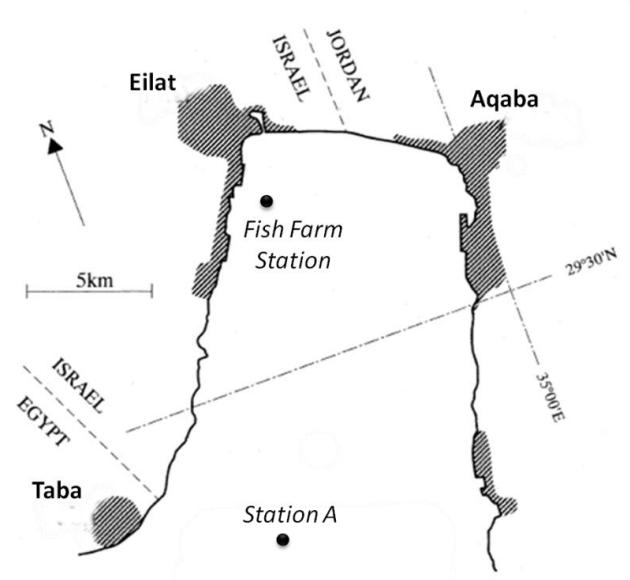

Fig. 3: *Location of the sampling points "Fish Farm Station" and "Station A"*

ANALYSIS OF TIME SERIES

At the beginning, the different time series were examined (nutrients, *chlorophyll a*, temperature and irradiance), and bivariate correlations between them were sought (*chlorophyll a* and temperature, *chlorophyll a* and each nutrient), with regression line and R^2 (Microsoft Excel), *Pearson's correlation coefficient* (R) and p-value (MATLAB software). Statistical analyzes were performed on the *chlorophyll a* time series to see if there were significant differences between the two sampling stations before and after the Fish Farm closure (t-test for dependent samples, STATISTICA software). Statistical analysis was also performed within each sampling station, to check if there were significant differences before and after the Fish Farm closure. The test was carried out for both the sampling stations for *chlorophyll a*, PO_4, NO_3 and $SiOH_4$ (t-test for independent samples, STATISTICA software). This step was crucial to understand how the data were linked to each other.

CONCEPTUAL DIAGRAM

A conceptual diagram was built containing the state variables, the forcing functions and how these components are interrelated (Fig. 4). In the present study *chlorophyll a* concentration and the phytoplankton sp. are the

state variables used to describe the state of the ecosystem. Forcing functions influence the state of the ecosystem. In this model the maximum growth rate of the state variable is limited by temperature, nutrient concentration and light available for the photosynthesis process. The other processes influencing algal dynamics (grazing, respiration, exudation, non-predatory mortality, and settling) are considered as functions of temperature.

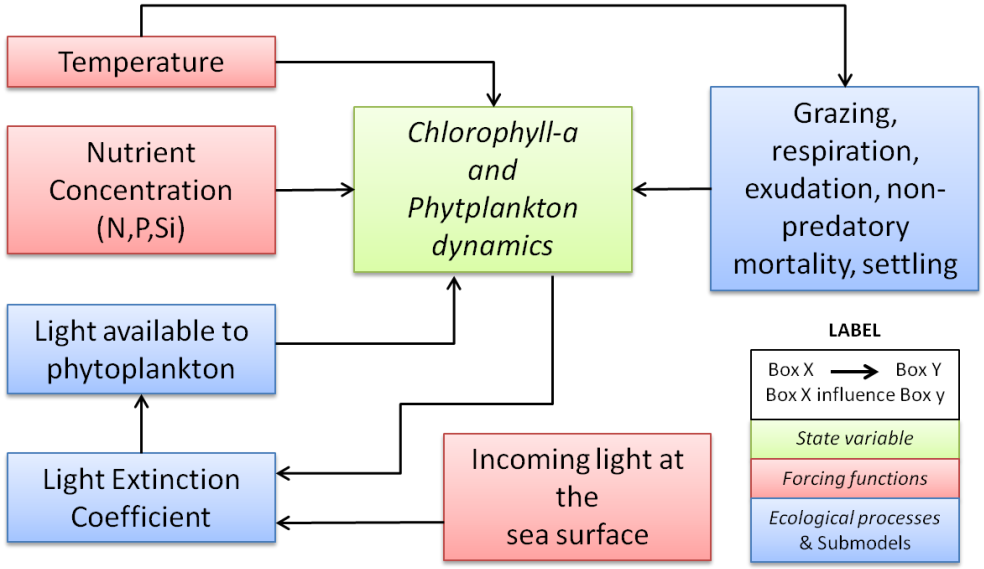

Fig. 4: C*onceptual model that show how forcing functions and ecological processes are interrelated for phytoplankton dynamics.*

MATHEMATICAL FORMULATION OF THE PROCESS

The equation which describes the algal growth was chosen to model the dynamics of *chlorophyll a* (Jørgensen and Bendoricchio 2001):

$$\frac{dA}{dt} = (\mu - r - es - m - s) \cdot A - G \qquad (1)$$

$\frac{dA}{dt}$ represents the variation in the *chlorophyll a* (A) concentration per day. In this differential equation A can either be the algal biomass or the *chlorophyll a* concentration. μ represents the gross growth rate $\left(\frac{1}{t}\right)$; r is the respiration rate $\left(\frac{1}{t}\right)$; es is the exudation rate $\left(\frac{1}{t}\right)$; m is the non-predatory mortality rate $\left(\frac{1}{t}\right)$; s is the settling rate $\left(\frac{1}{t}\right)$ and G is the loss due to grazing $\left(\frac{1}{t}\right)$. In this model it was decided to lump parameters r, es, m, s and G into a single loss parameter since this study is not aimed at discovering the cause of the loss in terms of *chlorophyll a*; moreover, quantifying the different

parameters would add unnecessary complexity to the model and require hitherto unavailable data. The parameter μ that represents the growth rate is usually modelled by the equation (Jørgensen and Bendoricchio 2001):

$$\mu = \mu_{max}(T_{ref}) \cdot f[f_1(T), f_2(L), f_3(N)] \quad (2)$$

This equation was chosen because it represents a classic, general and simple method for modelling phytoplankton dynamics. In this equation $\mu_{max}(T_{ref})$ is the maximum growth rate at the reference temperature T_{ref}. Whereas f is a function of the factors limiting growth. The value of $\mu_{max}(T_{ref})$ is achieved under optimal, non–limiting conditions, with perfect availability of light and nutrients. Functions $f_1(T)$, $f_2(L)$ *and* $f_3(N)$ represent the temperature relationship, the light limitation and the limitation of maximum growth rate due to nutrient starvation respectively.

Function $f_1(T)$ limits the $\mu_{max}(T_{ref})$ as a function of the water temperature. For this function two possible solutions were tried. It was possible to chose the usual *Arrhenius* exponential model (Jørgensen and Bendoricchio 2001):

$$f_1(T) = \vartheta^{(T-T_{ref})} \quad (3)$$

Where T is the temperature data, ϑ is a parameter and its value should range between 1 and 1.05. The variation of this parameter increases the influence of temperature on the *chlorophyll a* time trajectory (e.g. it exacerbates peaks); T_{ref} was assumed to be 24°C.

The temperature can also be modelled with the skewed normal distribution around an optimum temperature (Jørgensen and Bendoricchio 2001):

$$f_1(T) = e^{\left[-2.3\left(\frac{T-T_{opt}}{T_x-T_{opt}}\right)^2\right]} \quad (4)$$

Where T is the temperature data, $T_x = T_{min}$ if $T < T_{opt}$, $T_x = T_{max}$ if $T \geq T_{opt}$. T_{min} is the minimum temperature under which the growth is zero, T_{max} is the maximum temperature giving a non-zero growth, T_{opt} is the optimum temperature for the growth.

Function $f_2(L)$ that represents light limitation, in this case, is expressed as the measure of irradiance expressed in W/m². For this function two possible solutions were tried: the *Michaelis-Menten* equation, and the

Steel formulation. The *Michaelis-Menten* equation simulates a saturation effect of light (Jørgensen and Bendoricchio 2001):

$$f_2(L) = \frac{L}{k_L + L} \tag{5}$$

Where k_L is the semisaturation constant and L is the light intensity useful for photosynthesis, defined by the following equation (Jørgensen and Bendoricchio 2001):

$$L = \alpha \cdot I_0 \cdot e^{-\gamma \cdot h} \tag{6}$$

α represents a coefficient that accounts for photosynthetic activity, namely $\alpha = 0.56$, I_0 is the light intensity at the surface (W/m²), γ is the extinction coefficient in water body (0.035 m^{-1}) and h is the water depth (m) (Hill 1963, Jørgensen and Bendoricchio 2001).

The second light limitation model is an optimum curve, or *Steel formulation* (Jørgensen and Bendoricchio 2001)*:*

$$f_2(L) = \frac{L}{L_{opt}} e^{\left(1 - \frac{L}{L_{opt}}\right)} \tag{7}$$

Where L is the light intensity usabal for photosynthesis, L_{opt} is the optimum light intensity for photosynthesis, this value can be modified according to the acclimation of phytoplankton to light variation at depth and time.

Function $f_3(N)$ represents the limitation by nutrient availability. For this function the *Michaelis-Menten* kinetics or *Monod* approach was chosen, where the $\mu_{max}(T_{ref})$ is limited by the external concentration of the nutrient (Jørgensen and Bendoricchio 2001):

$$f_3(N) = \frac{N}{k_N + N} \tag{8}$$

N represents the external concentration of nutrient expressed in micromol/l, k_N represents the semi-saturation constant. The semi-saturation constant k_N is the nutrient concentration at which the reaction rate is at its half-maximum. It is a measure of the algal affinity for nutrients, which is linked to phytoplankton growth and, thus, to *chlorophyll a* production. A low value of k_N and an high value of k_N indicate high and low affinities respectively. If there was inserted more than one nutrient in the model, several possibilities of interaction were tested using *multiplication*, *arithmetic*

mean, *harmonic mean* and *minimum of Liebig* (Jørgensen and Bendoricchio 2001).

Several models were tried for testing and comparing different forecast scenarios and understanding which forces determine phytoplankton dynamics. The models were made with different combinations of nutrients:

- without any nutrient (only temperature);
- with PO_4 only;
- with NO_3 only;
- with $SiOH_4$ only;
- with PO_4 and SiO_4;
- with NO_3 and PO_4;
- with NO_3, PO_4 and SiO_4;
- with different nutrients until and after the closure of the Fish Farm;

with different time scales to understand if it is better to use a model that considers or ignores the Fish farm closure:

- three years;
- prior and following the Fish Farm closure;

and with different k_N constants to understand if the *Fish Farm Station* closure produced a significant change in phytoplankton community composition or not (it is assumed that different constants correspond to different phytoplankton species):

- k_N remains the same over three years of simulation;
- k_N changes after the Fish Farm closure.

TRANSFER TO COMPUTER

To build the model, the MATLAB software was used (version 7.6.0.324 R2008a), in particular a tool named *Simulink*. *Simulink* is an environment for multidomain simulation and Model-Based Design for dynamic and embedded systems.

VERIFICATION

Verification of the model was performed. It is a subjective assessment of the behaviour of the model, to test its internal logic. The

values of the parameters were changed, one by one, to see if the model reacted as expected and if it was stable in the long term (Jørgensen and Bendoricchio 2001).

SENSITIVITY ANALYSIS

Sensitivity analysis was carried out by changing the parameters, forcing functions, initial values and submodels, and observing the corresponding response in the state variable. This is a fundamental step to learn the proprieties of the model, since through this analysis it is possible to get a good overview of the most sensitive components and processes in the model. The sensitivity of any one parameter was defined by the following equation (Jørgensen and Bendoricchio 2001):

$$S = [\partial x/x]/[\partial P/P] \quad (9)$$

Where S is the sensitivity, P is a parameter, and x is the state variable (*chlorophyll a*). The values of parameters were changed, one by one, by +2% and -2%. It was chosen to change the parameters by +2% and -2% because the models were extremely sensitive to larger changes of some of the parameters.

CALIBRATION

Calibration is an attempt to find the best agreement between computed and observed data by varying some selected parameters. The aim of calibration is to improve data fit through parameter estimation. In this model the parameters found in the literature, which referred to ecosystems similar to that of the Gulf of Aqaba, were considered just as approximate, starting values. Initially, in this model, calibration was performed manually, followed by an automatic calibration using *Simulink* (MATLAB). The automatic calibration provides a graphical user interface for estimating the parameters and initial states of the model using empirical input and output data pairs.

VALIDATION

Validation consisted of testing the selected parameters for the *Fish Farm Station* with an independent set of data, in this specific case referring to the sampling *Station A* in the northern Gulf of Aqaba. This operation is useful for testing if the model is replicable or if the model is valid only for the *Fish Farm Station*. After validation the differences between the various *Fish Farm Station* and *Station A* models was assessed.

CONFRONTING MODELS

Different models were compared by three indexes: Residual Sum of Squares (RSS), Nash–Sutcliffe Model Efficiency Coefficient (E) and Akaike Information Criterion (AIC) (Akaike 1974, Moriasi et al. 2007, Nash and Sutcliffe 1970).

Residual Sum of Squares (RSS) is a measure of the discrepancy between the data and the estimation of the model. The index is the sum of squares of residuals. The residuals are the difference between the sample and the estimated data:

$$RSS = \sum_{t=1}^{T} (Q_m^t - Q_o^t)^2 \quad (10)$$

Where Q_m^t is modelled data at time t, Q_o^t is observed data of chlorophyll a at time t. The closer the RSS value is to 0 the more accurate the model is.

The Nash–Sutcliffe Model Efficiency Coefficient (E) was used to assess the predictive power of the models:

$$E = 1 - \frac{\sum_{t=1}^{T}(Q_m^t - Q_o^t)^2}{\sum_{t=1}^{T}(Q_o^t - \overline{Q_o})^2} \quad (11)$$

Where Q_m^t is modelled data at time t, Q_o^t is observed data of *chlorophyll a* at time t, $\overline{Q_o}$ is the average of observed data (Moriasi et al. 2007, Nash and Sutcliffe 1970). This index can range from $-\infty$ to 1, if $E = 1$ there is a perfect match between modelled data to the observed data. If $E = 0$ the model predictions are as accurate as the mean of the observed data. If $E < 0$ the residual variance (described by the numerator) is larger than the data variance (described by the denominator), the closer E is to 1 the more accurate the model is. Since all models were applied to the same dataset of

observed *chlorophyll a* data, the denominator of E was constant and, thus, the use of E was perfectly equivalent to using RSS, as can be appreciated by comparing equations (10) and (11).

The Akaike Information Criterion (AIC) measures the relative goodness of fit (Akaike 1974). This index includes a penalty that is an increasing function of the number of estimated parameters; this measure is particularly important because equations (10) and (11) do not take into account the number of parameters (Akaike 1974):

$$AIC = \chi^2 + 2k \tag{12}$$

Where k is the number of parameters and χ^2 is the Chi-squared distribution:

$$\chi^2 = M \cdot ln\left(\frac{\sum(Q_m^t - Q_0^t)^2}{M}\right) \tag{13}$$

Where M is the number of sampled points, Q_m^t is modelled data at time t, Q_0^t is observed data of *chlorophyll a* at the time t. The more negative the AIC index value is, the more accurate the model is. If the difference in the AIC value, between two models, is less than two they are roughly equivalent (Akaike 1974).

RESULTS

ANALYSIS OF TIME SERIES

At the beginning it was necessary to analyze and understand the time series of the principal factors that control the ecosystem in question. The time series of the principal factors that can drive phytoplankton dynamics are shown in Fig. 5, Fig. 6, Fig. 7, Fig. 9, Fig. 10 and Fig 11.

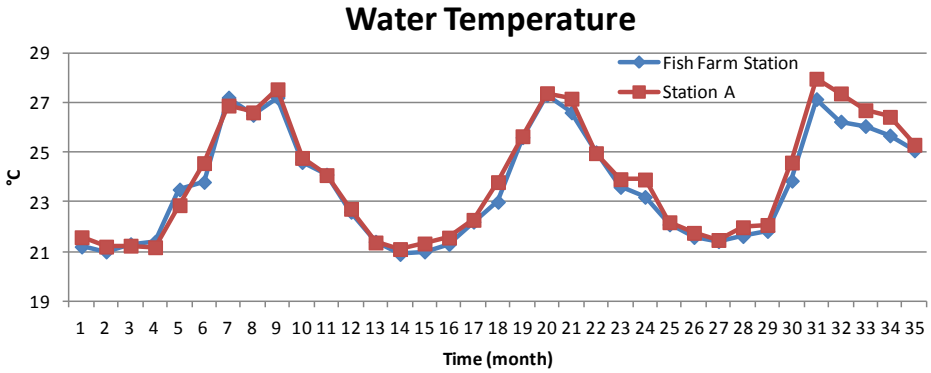

Fig. 5: *time series of the water temperature (°C) sampled at 1-m depth; in the abscissa "time 1" corresponding to the first month of sampling (14th January 2007) and "time 35" the last month (28th December 2009).*

In the time series of the water temperature there were no evident differences between the *Fish Farm Station* data and *Station A* data. In both sampling stations the seasonality of this forcing function can be seen: high temperature in the summer-fall months and low temperature in the winter-spring months.

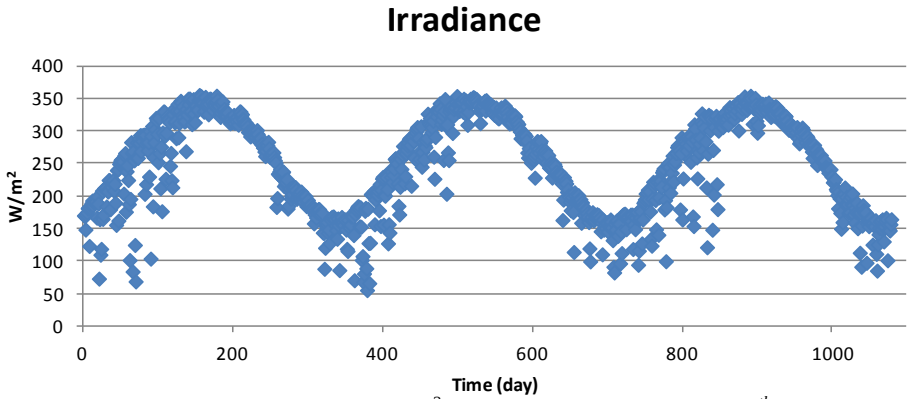

Fig. 6: *time series of the irradiance (W/m^2) sampled every day from 14th January 2007 to 28th December 2009 in the Interuniversity Institute for Marine Science (IUI), Eilat.*

In this graph the sunlight irradiance (W/m^2) was represented, these data were used for both the sampling stations. The same seasonal trend can be seen, similar to the pattern of the water temperature (Fig. 5).

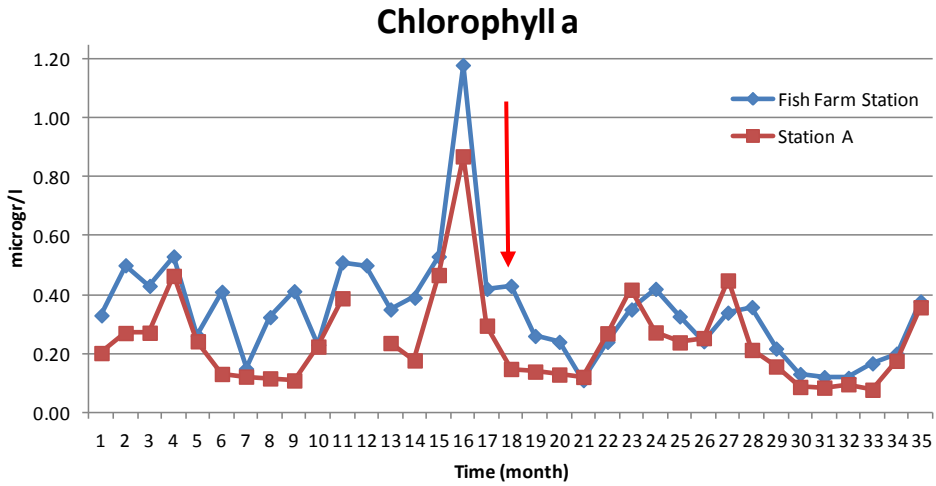

Fig. 7: *time series of the chlorophyll a concentration (microgr/l) sampling from 14th January 2007 in both the sampling stations.*

Figure 7 shows the time series of *chlorophyll a* concentration measurements. The red arrow, in this graph and in all the following graphs, indicates the 17th June 2008, the date of the complete closure of the Fish Farm. It is possible to see how before the closure of the Fish Farm the concentration of *chlorophyll a* in the *Fish Farm Station* was significantly different from its concentration in *Station A* (t-test for dependent samples: *t=6.57; p<0.0001*). From the point indicated by the red arrow to the end of the time series, the *chlorophyll a* data of *Station A* and *Fish Farm Station* appear to become more similar (t-test for dependent samples: *t=1.95; p=0.069854*).

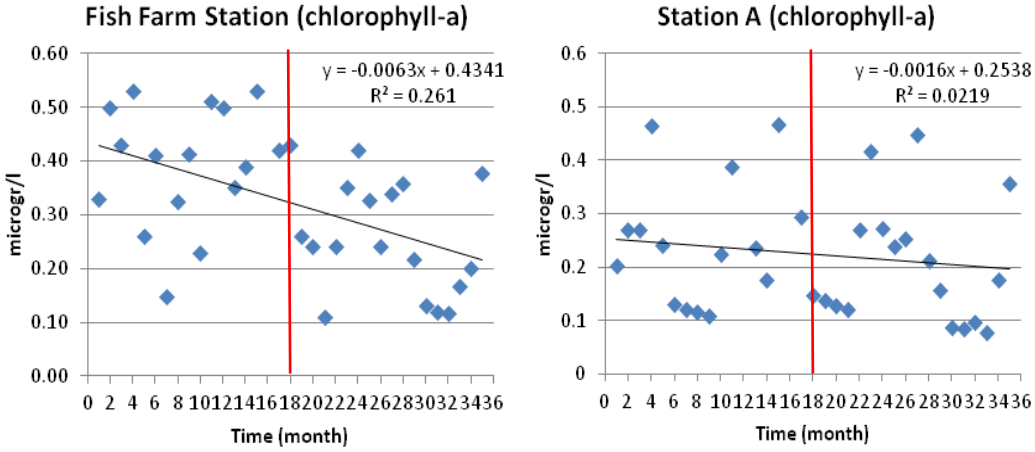

Fig. 8: *The two graphs show the time series of chlorophyll a with the regression line (indicating the trend over time) and R^2, for both sampling stations. The red line indicates the Fish Farm closure.*

In Fig. 8 the outlier in *chlorophyll a* data was deleted for month 16, because it excessively influenced the regression line. The same procedure was

applied to the graphs below that include a regression line (Fig. 12, Fig 13, Fig. 14 and Fig. 15). The first graph of Fig. 8 shows how, in the *Fish Farm Station*, the *chlorophyll a* trend decreases over time (*Pearson's correlation coefficient* (R) R=-0.51, *p=0.0019*), in particular the concentration decreased after the Fish Farm closure. Indeed there is a significant difference in *chlorophyll a* before and after the Fish Farm closure (t-test for independent samples: *t=3.13; p=0.007*). In the *Station A* graph there is a small decrease in *chlorophyll a* over time (R=-0.09, *p=0.5962*) but it is not as strong as in the *Fish Farm Station* and there are no significant differences (t-test for independent samples: *t=0.97; p=0.075*).

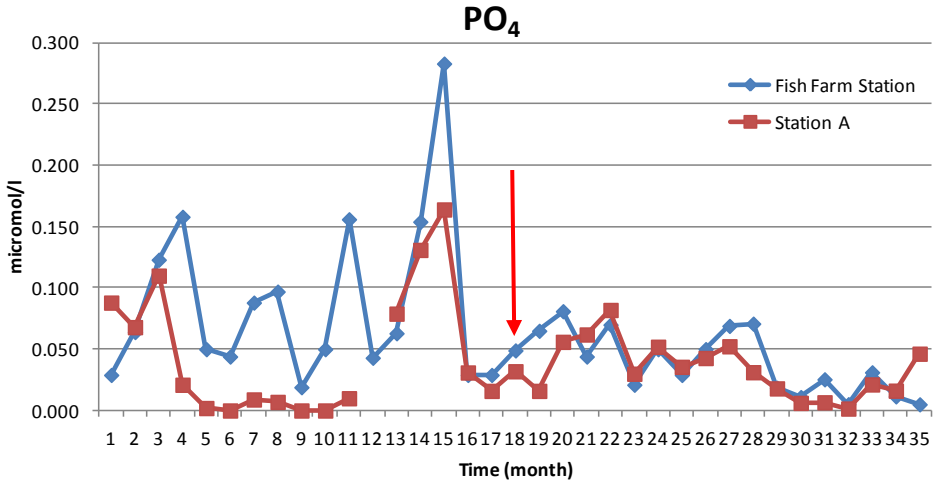

Fig. 9: *Time series of PO_4 concentration (micromol/l) from 14th January 2007 at both sampling stations.*

It is evident that before the Fish Farm closure , the concentration of PO_4 was higher in the *Fish Farm Station* than it was in *Station A*. After the Fish Farm closure the trend and concentrations of PO_4 became more similar in both sampling stations. The statistical analysis of the *Fish Farm Station* data reveals that there are significant differences before and after the Fish Farm closure (t-test for independent samples: *t=2.67; p=0.000564*). In the *Station A* data there are significant differences before and after the red arrow (t-test for independent samples: *t=0.53; p=0.002352*).

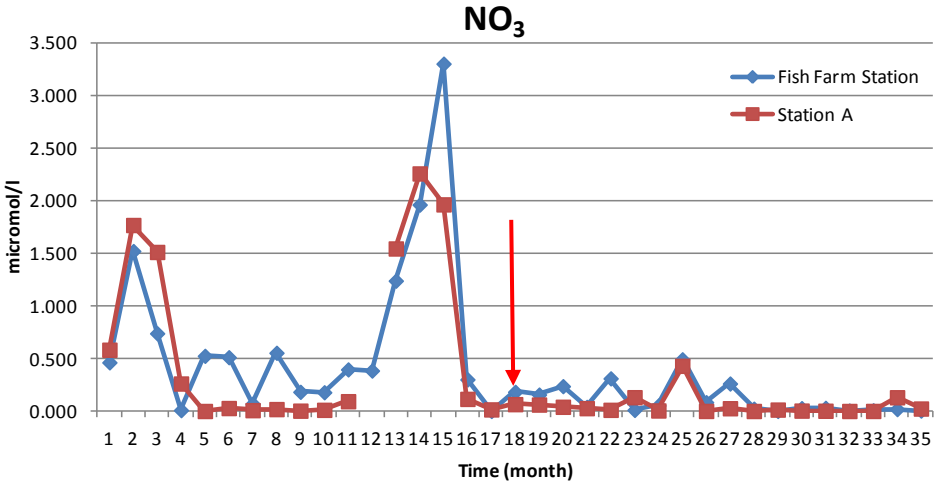

Fig. 10: *Time series of the NO_3 concentrations (micromol/l) from 14th January 2007 in both sampling stations.*

Both nitrate concentrations and peaks thereof at both stations were higher before the closure of the farm than during the following period. For both station data-sets the statistical analysis shows a significant difference before and after the red arrow (t-test for independent samples *Fish Farm Station*: $t=2.70$; $p<0.0001$ and *Station A*: $t=2.59$; $p<0.0001$). Also, the time series show that concentrations next to the Fish Farm were higher than in the open sea, a difference that disappeared later on.

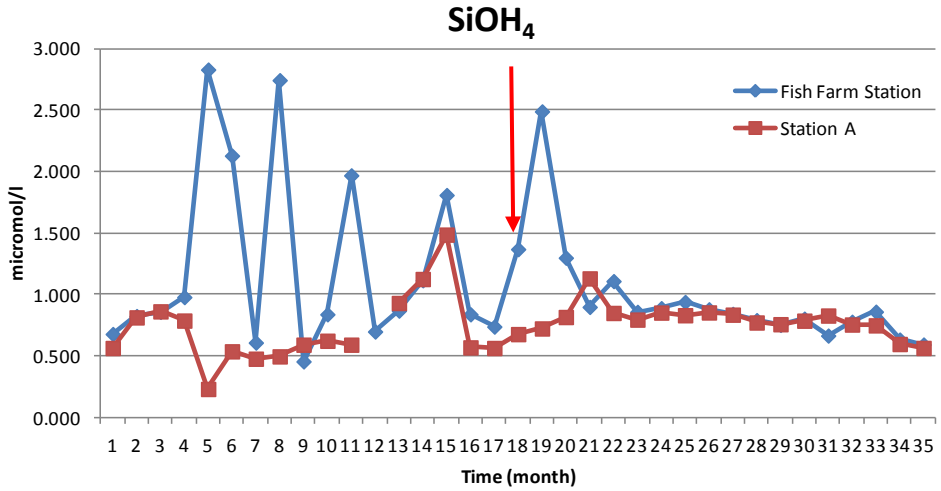

Fig. 11: *time series of the $SiOH_4$ (micromol/l) sampling from 14th January 2007 in both sampling stations.*

In the silicate graph the pattern of $SiOH_4$ is very different at the two sampling stations: before the red arrow in the *Fish Farm Station* data there are a short, strong fluctuations compared to *Station A* data. About three months after the Fish Farm closure such fluctuations were no longer

observed, and the trend of $SiOH_4$ became similar in the two sampling stations (in the *Fish Farm Station* the concentration average is higher before the Fish Farm closure, in *Station A* it is higher after the closure). In both datasets there were significant differences before and after the Fish Farm closure (t-test for independent samples *Fish Farm Station*: *t=2.33*; *p<0.0001* and *Station A*: *t=-1.23*; *p=0.001605*).

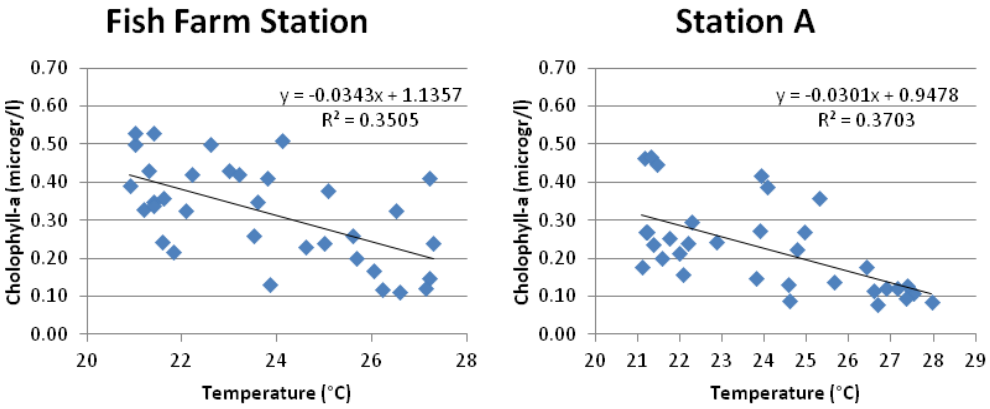

Fig. 12: *Time series of chlorophyll a concentration (micromol/l)as function of the water temperature (°C), both data sets were collected from 14th January 2007.*

In these two graphs the *chlorophyll a* data is shown as a function of temperature that was measured in the *Fish Farm Station* and *Station A*. Both graphs show how the *chlorophyll a* concentration decreases with increasing temperature (*Pearson's correlation coefficient* (R) is similar in the *Fish Farm Station* R=-0.59, *p=0.00022684* and *Station A* R=-0.61, *p=0.00012417*). In both *chlorophyll a* datasets an outlier datum in the 16th month was deleted (1.18 microgr/l in the *Fish Farm Station* and 0.87 microgr/l in the *Station A*). The same procedure was applied to the following graphs.

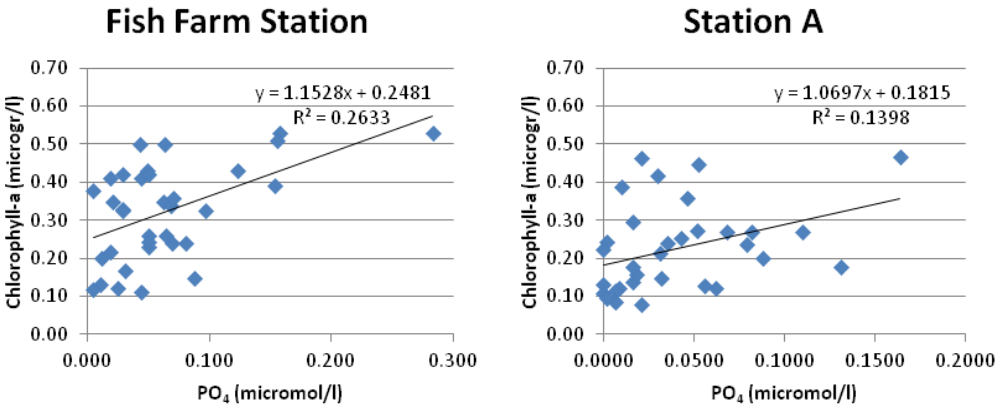

Fig. 13: *Time series of chlorophyll a concentration (microgr/l) as function of PO_4 concentration (micromol/l). Both data sets were collected from 14th January 2007.*

These two graphs show the sampled *chlorophyll a* data as function of the PO_4 data: an increase in PO_4 concentration entails an increase in the phytoplankton population and, as a consequence, an increase in detected *chlorophyll a*. In both stations there is a positive correlation, which is stronger in the Fish Farm Station (R=0.51, *p=0.0019*) than in Station A (R=0.38, *p=0.0271*).

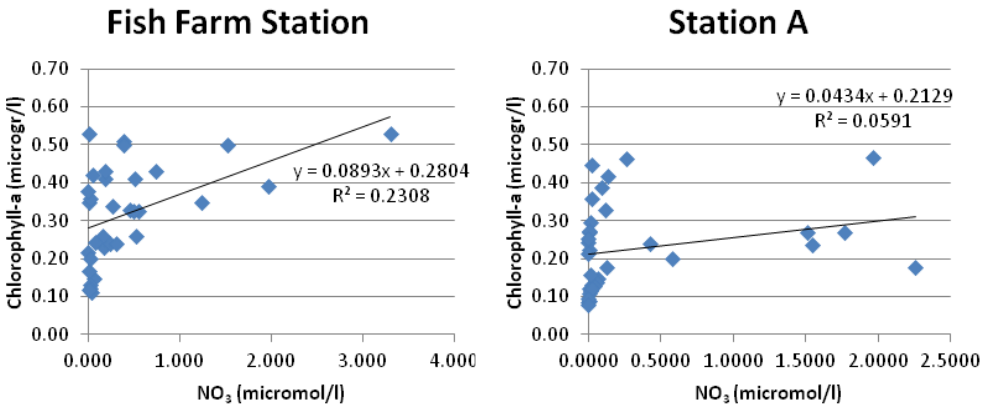

Fig. 14: *Time series of chlorophyll a (microgr/l) as a function of NO_3 concentratioon (micromol/l., Both data sets were collected from 14th January 2007.*

The first graph shows the correlation between the field measure of *chlorophyll a* and NO_3 in the *Fish Farm Station* (R=0.46, *p=0.0064*). The second graph shows the same correlation, but concerning the data collected in *Station A* (R=0.24, *p=0.1655*). A negative correlation can be seen in both sampling stations, which is more marked in the *Fish Farm Station*.

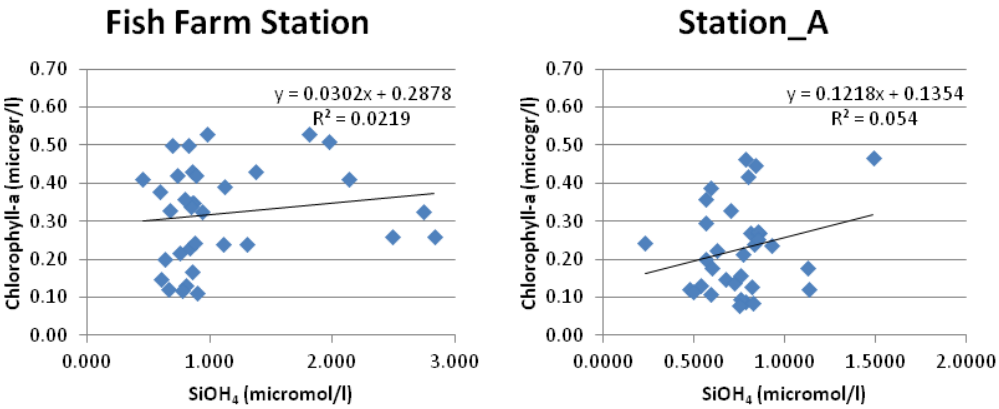

Fig. 15: *Time series of the chlorophyll a concentration (microgr/l) as a function of $SiOH_4$ (micromol/l). both data sets collected from 14th January 2007.*

These two graphs show the correlation between $SiOH_4$ and *chlorophyll a* (*Fish Farm Station* R=0.15, *p=0.4034*; *Station A* R=0.23, *p=0.1860*).

SIMULATION OF THE *FISH FARM STATION* MODELS

Verification (p. 12) showed how the variation of parameters implied a change in the *chlorophyll a* simulation.

Increasing the constant:

- "μ_{max}" (2), *chlorophyll a* simulated concentration increases over time
- " G " (1), *chlorophyll a* simulated concentration decreases over time
- "T_{ref}" (2), *chlorophyll a* simulated concentration increases over time
- "k_L" (5), *chlorophyll a* simulated concentration decreases over time
- "k_N" (8), *chlorophyll a* simulated concentration decreases over time
- " ϑ " (3), increases in the maximum value of *chlorophyll a* concentrations, simultaneously decreases in the minimum value of *chlorophyll a* concentrations.

Decreasing the constant:

- "μ_{max}" (2), *chlorophyll a* simulated concentration decreases over time;
- " G " (1), *chlorophyll a* simulated concentration increases over time;
- "T_{ref}" (2), *chlorophyll a* simulated concentration decreases over time;
- "k_L" (5), *chlorophyll a* simulated concentration increases over time;
- "k_N" (8), *chlorophyll a* simulated concentration increases over time;

- " ϑ " (3), decreases in the maximum value of *chlorophyll a* concentrations, simultaneously increases in the minimum value of *chlorophyll a* concentrations.

Changing the constant:

- "T_{opt}" (4), *chlorophyll a* simulated concentration greatly increases in correspondence to the T_{opt} value;
- "L_{opt}" (7), *chlorophyll a* simulated concentration greatly increases in correspondence to the L_{opt} value.

The sensitivity analysis (p. 12) shows that the parameters that most strongly influence the *chlorophyll a* simulated values are k_N, k_L, μ_{max} and G. This finding means that the preview constants compared to the others are more sensitive to small variations. Hence, small changes in one or more of these four constants cause great changes in the *chlorophyll a* simulated trend.

All the following tables show some models with the number of parameters, the results of Residual Sum of Squares (RSS), the Nash–Sutcliffe Model Efficiency Coefficient (E) and the Akaike Information Criterion (AIC). Abbreviations represent the processes found in the model. In all the abbreviations of the models the forcing functions of grazing, respiration, exudation, non-predatory mortality and settling were omitted because these parameters were included in all the models. *Station A chlorophyll a* time series (Fig. 7) shows how the *chlorophyll a* values stay low during the summer months and increase during the winter months, as described in the typical Gulf of Aqaba phytoplankton dynamics (Al-Najjar et al. 2007, Mackey et al. 2007, Mackey et al. 2009). Conversely, in the *chlorophyll a Fish Farm Station* time series (Fig. 7) low *chlorophyll a* concentrations cannot be seen in the summer months but concentrations are high in winter, thus the typical phytoplankton seasonality dynamic is lessened, presumably by the nutrient input from the fish exreta and decomposing food residues before the Fish Farm closure. For this reason it was chosen to not apply a seasonal pattern to the *Fish Farm Station* simulation models.

Table 1 summarizes the results for 8 simple models for the *Fish Farm Station*. In these models the additional forcing functions are temperature (with *optimum* (4) or *Arrhenius* (3) function) and only one nutrient (with *Michaelis-Menten* (8) function) selected from NO_3, PO_4 and $SiOH_4$. Abbreviations indicate which parameters are inserted in the model:

	N°Parameters	RSS	E	AIC
T°(OPT)	8	4.21	-2.366	-58.123
T°(EXP)	6	1.333	-0.066	-102.381
T°(OPT)_NO_3	9	2.129	-0.703	-79.981
T°(EXP)_NO_3	7	1.024	0.181	-109.614
T°(OPT)_PO_4	9	1.787	-0.429	-86.117
T°(EXP)_PO_4	7	1.084	0.133	-107.614
T°(OPT)_$SiOH_4$	9	2.333	-0.866	-76.782
T°(EXP)_$SiOH_4$	7	1.299	-0.038	-101.286

Table 1

T°(OPT): a model with only temperature to regulate the dynamics of *chlorophyll a*; "OPT" indicates that the function selected for the model was the *optimum* function.

T°(EXP): a model with only temperature to regulate the dynamics of *chlorophyll a*; "EXP" indicates that the function selected for the model was the *Arrhenius* function.

In the other models of *Table 1*, after the temperature function, there is the nutrient that regulates the simulated dynamics of *chlorophyll a* (NO_3, PO_4 or $SiOH_4$).

In all models it can be seen how the *Arrhenius* relation for the temperature function is much better than the *optimum* formulation. For that reason in the following model, the exponential relation for the temperature function *(Arrhenius)* was applied.

The following graph shows the time series simulations of model **T°(EXP)** and the models that result in the best simulations *(Table 1)*: **T°(EXP)_NO_3** and **T°(EXP)_PO_4**. In this and all following graphs, the blue line represents the simulated data and the blue dots represent the real sampled data.

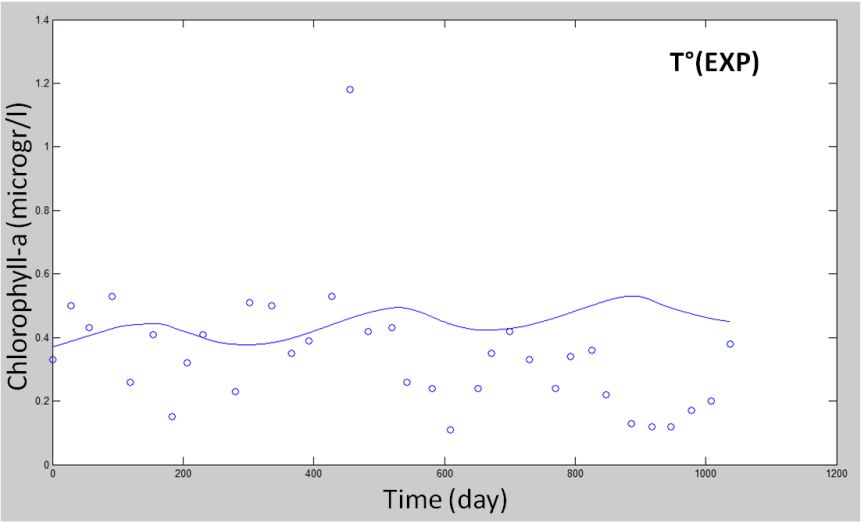

Simulation Graph 1

The *Simulation Graph 1* shows how the dynamics of *chlorophyll a* is similar over the three years. This is because, in this model, the dynamics of *chlorophyll a* is modelled by only the temperature forcing function and this function follows the seasonal water temperature data (Fig. 5).

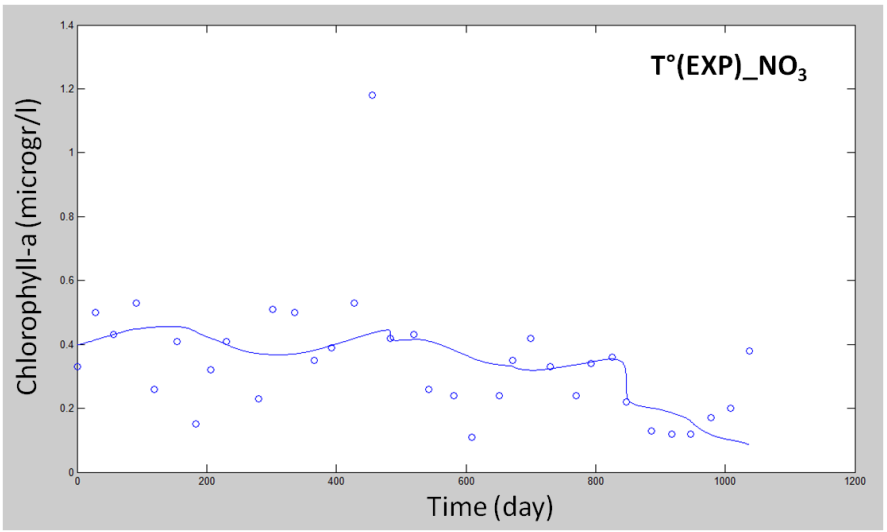

Simulation Graph 2

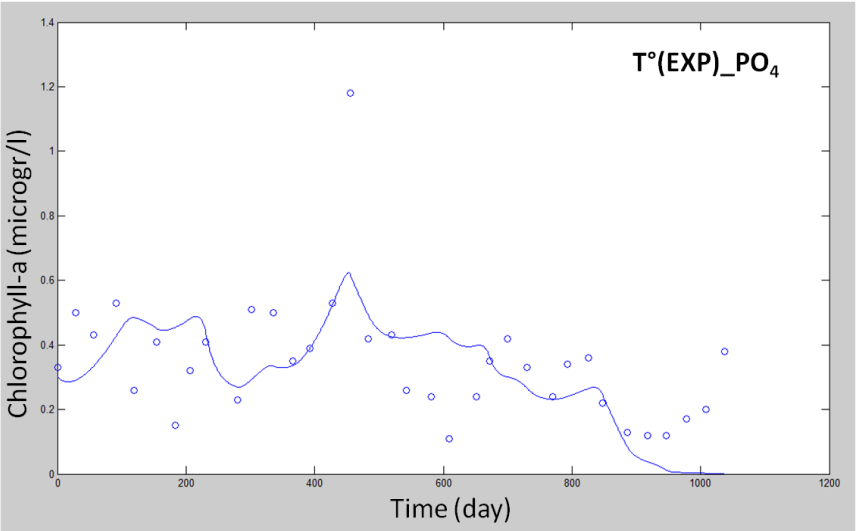

Simulation Graph 3

Simulation Graph 2 and *Simulation Graph 3* show the simulation with the addition of NO_3 or PO_4. The results of simulations improve in both conditions and the trend changes year by year, which is due to the interaction between the temperature forcing function and the nutrient forcing function.

Table 2 shows some models with various combinations of nutrients. The function of temperature with the *Arrhenius* function is inserted in all these models (indicated with T°).

	N°Parameters	RSS	E	AIC
T°_PO_4_X_NO_3	8	0.998	0.202	-108.519
T°_PO_4_NO_3_$SiOH_4$_liebig	9	1.759	-0.406	-86.672
T°_PO_4_NO_3_liebig	8	1.645	-0.315	-91.027
T°_NO_3_kvar	8	0.883	0.294	-112.776
T°_PO_4_kvar	8	1.077	0.139	-105.836
T°_NO_3_BFC_PO_4_PFC	8	0.842	0.327	-114.477
T°_PO_4_BFC_NO_3_PFC	8	1.262	-0.009	-100.294
T°_NO_3_X_$SiOH_4$_BFC_PO_4_PFC	9	1.318	-0.054	-96.772
T°_NO_3_BFC_$SiOH_4$_PFC	8	0.824	0.341	-115.228

Table 2

T°_PO_4_X_NO_3: the *Michaelis-Menten* function for PO_4 and NO_3 was inserted in this model. The values of the *Michaelis-Menten* function for the nutrients

are multiplied at every time step of the model (the multiplication in the *Table 2* is indicated by "X"):

$$f_{3a}(PO_4 \times NO_3) = \frac{PO_4}{k_P + PO_4} \times \frac{NO_3}{k_N + NO_3} \quad (14)$$

The function applied in this model is a variation of equation (8), where PO_4 indicates the PO_4 data at time t, NO_3 indicates the NO_3 data at time t, k_P the semi-saturation constant for PO_4 and k_N the semi-saturation constant for NO_3.

T°_PO_4_NO_3_$SiOH_4$_liebig: the minimum of the Liebig Law to define the limiting nutrient for each simulation time of the model was inserted: the model chose the lowest value of the results of three functions (8), one for each nutrient.

T°_PO_4_NO_3_liebig: this model is the same as the previous one but without $SiOH_4$ data.

T°_NO_3_kvar and T°_PO_4_kvar: these two models have one nutrient each (NO_3 or PO_4) to regulate the phytoplankton dynamics. The (k_N) in the function (8) is the only parameter that can change after the *Fish Farm Station* closure. This is the first model where an ecological change due to the Fish Farm closure was simulated.

T°_NO_3_BFC_PO_4_PFC and T°_PO_4_BFC_NO_3_PFC: in the first model NO_3 limits the phytoplankton growth rate before the Fish Farm closure and PO_4 limits the growth rate after the Fish Farm closure. In the second model there is the opposite situation: PO_4 limits the growth rate before and NO_3 limits the phytoplankton growth rate after the Fish Farm closure. These models and the two models below were made to understand if the Fish Farm activity might have caused a change in the phytoplankton dynamics, resulting from the nutrients that regulate it. Therefore, a nutrient or nutrients were added before the Fish Farm closure and a different condition was found after the Fish Farm closure.

T°_NO_3_X_$SiOH_4$_BFC_PO_4_PFC: here NO_3 and $SiOH_4$ limits the growth before the Fish Farm closure, the values for the nutrients function are multiplied at each time. After the Fish Farm closure PO_4 begins to limit the phytoplankton growth.

T°_NO_3_BFC_$SiOH_4$_PFC: in this model NO_3 limits the growth rate before the Fish Farm closure and $SiOH_4$ limits the phytoplankton growth after the Fish Farm closure.

The following graph shows the time series simulations of the models that have the best results (*Table 2*) from the index (RSS, E and AIC): **T°_PO_4_X_NO_3**, **T°_NO_3_kvar**, **T°_PO_4_kvar**, **T°_NO_3_BFC_PO_4_PFC** and **T°_NO_3_BFC_$SiOH_4$_PFC**.

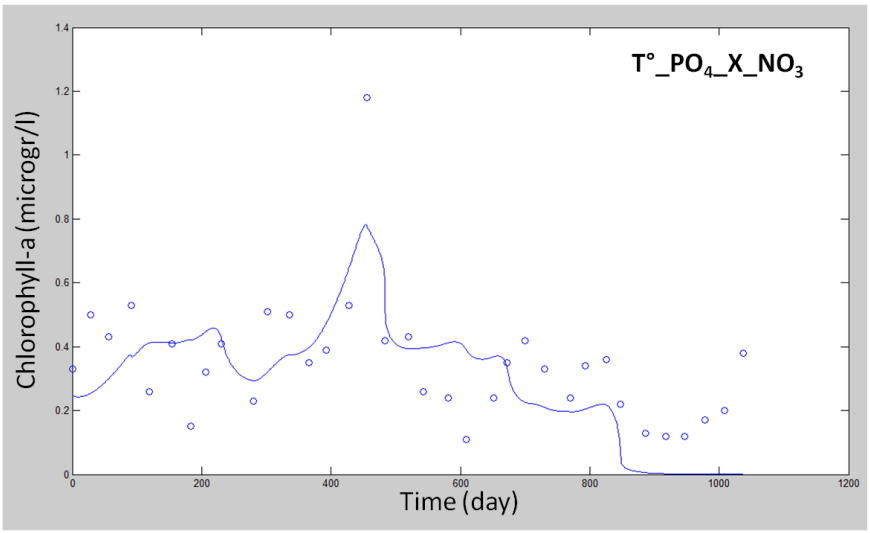

Simulation Graph 4

Simulation Graph 4 shows the interaction between two nutrients, PO_4 and NO_3. In this *Simulation Graph* there is no influence by the Fish Farm closure.

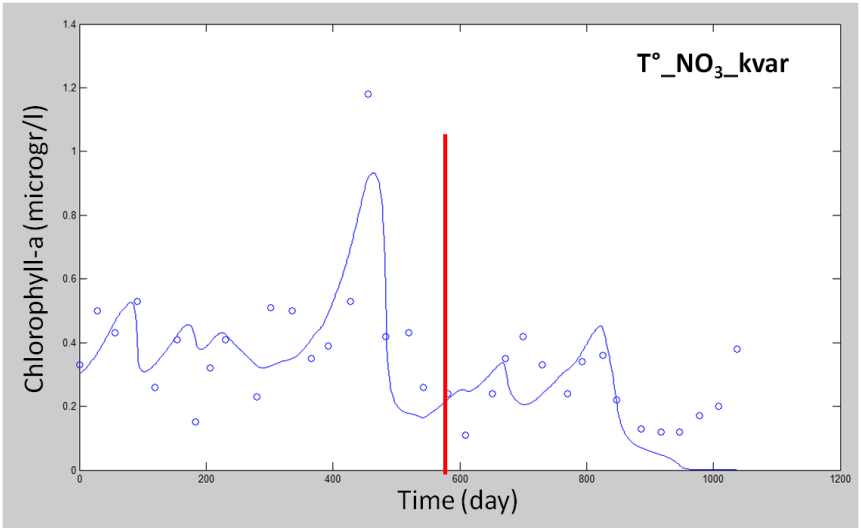

Simulation Graph 5

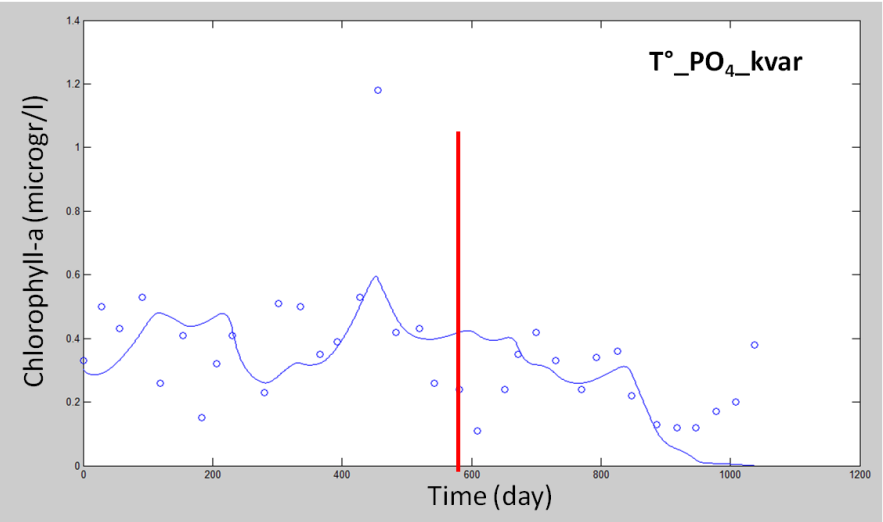

Simulation Graph 6

Simulation Graph 5 and *Simulation Graph 6* are the first simulations that include the semi-saturation constant (k_N) variation of the *Michaelis-Menten* function for the nutrient after the Fish Farm closure. In those and the following *Simulation Graph* the time when there is a change in k_N is represented by the red line.

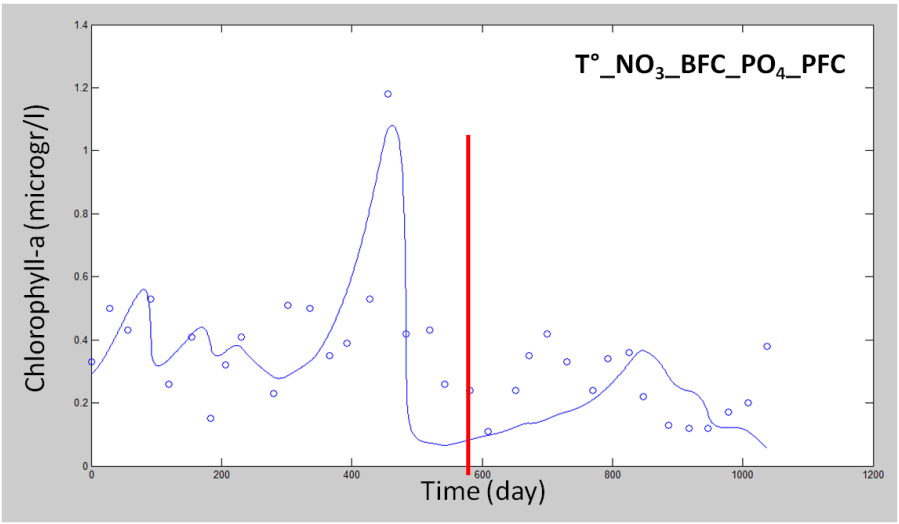

Simulation Graph 7

Simulation Graph 7 simulates a variation of the nutrients that regulate the phytoplankton dynamics: before the Fish Farm closure NO_3 is limiting and after PO_4 is limiting.

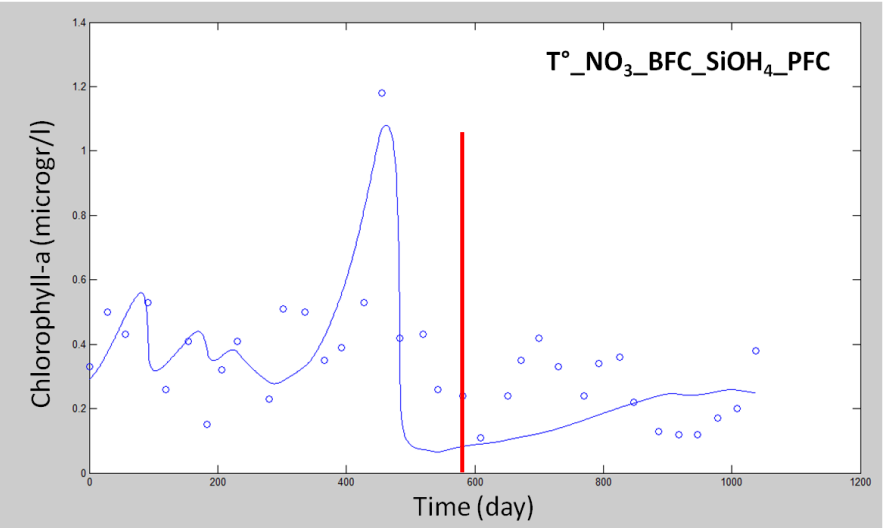

Simulation Graph 8

Simulation Graph 8 simulates a variation of the nutrients that regulate the phytoplankton dynamics: before the red line NO_3 is limiting and after $SiOH_4$ is limiting.

Table 3 shows models with the addition of the light limiting function (5) and (7):

	N°Parameters	RSS	E	AIC
T°_LIGHT_SATURATION	7	1.308	-0.046	-101.036
T°_LIGHT_OPTIMUM	7	4.034	-2.225	-61.624
T°_NO_3_kvar_LIGHT_SATURATION	9	0.706	0.435	-118.62
T°_NO_3_kvar_LIGHT_OPTIMUM	9	3.555	-1.842	-62.046
T°_NO_3_BFC_PO_4_PFC_LIGHT_ SATURATION	9	0.693	0.446	-119.29
T°_NO_3_BFC_PO_4_PFC_LIGHT_OPTIMUM	9	1.446	-0.156	-93.537
T°_NO_3_BFC_$SiOH_4$_PFC_LIGHT_ SATURATION	9	0.725	0.42	-117.698
T°_NO_3_BFC_$SiOH_4$_PFC_LIGHT_OPTIMUM	9	1.314	-0.05	-96.892

Table 3

Table 3 shows how the addition of the light function improves the models; this is evident in the AIC value, which also takes into account the increase in the number of parameters (see *Table 1* and *Table 2*). The table also highlights how the *Michaelis-Menten* function (saturation) for light is better than the *Steel formulation* (optimum). *Table 3* also includes the best model obtained for the *Fish Farm Station* data:

T°_NO_3_BFC_PO_4_PFC_LIGHT_SATURATION, in this simulation it was assumed that nitrogen regulates the phytoplankton dynamics before the Fish Farm

closure and that phosphate regulates the phytoplankton dynamics after the Fish Farm closure.

The following graphs show simulations of the models reported in *Table 3*. The following simulation displays differences between the saturation function (*Michaelis-Menteen*) and the *optimum* function (*Steel Formulation*).

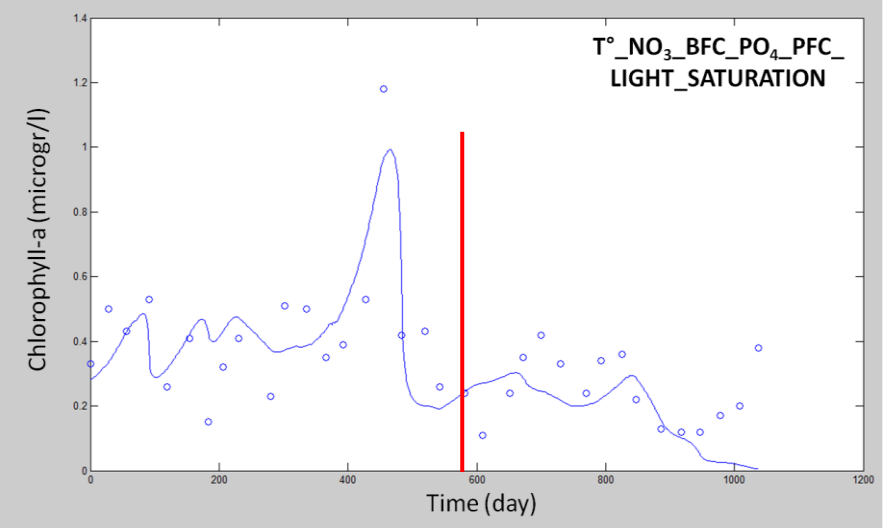

Simulation Graph 9

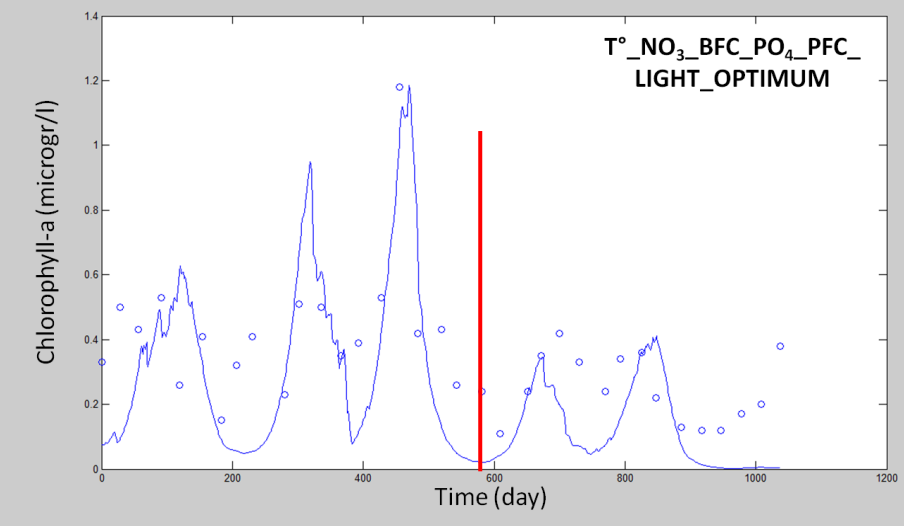

Simulation Graph 10

Simulation Graph 9 and *Simulation Graph 10* give different results with similar models that include NO_3 before the Fish Farm closure and PO_4 after

the Fish Farm closure. The light function is the only difference between the two models (*saturation* and *optimum*).

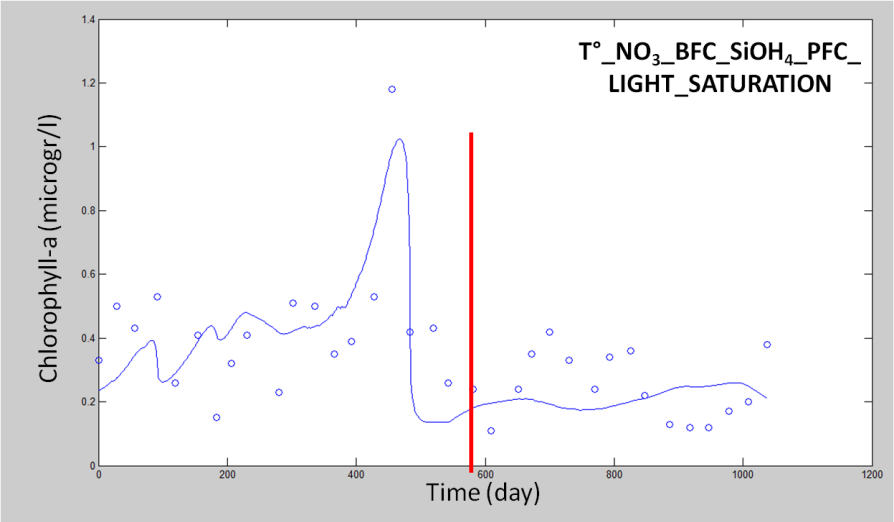

Simulation Graph 11

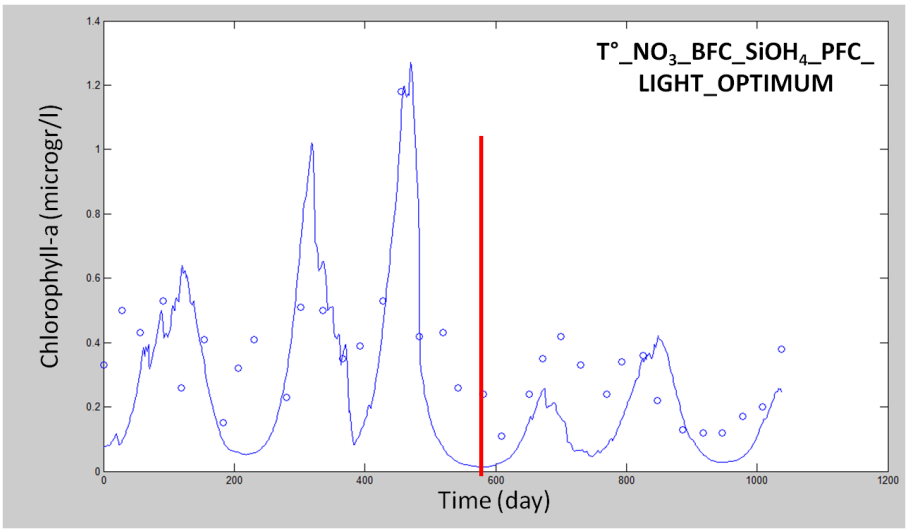

Simulation Graph 12

Simulation Graph 11 and *Simulation Graph 12* show two simulations of the model that includes NO_3 as limiting nutrient before the Fish Farm closure and $SiOH_4$ as limiting nutrient after the Fish Farm closure. The only difference between these graphs is again the light function.

Table 4 shows models with different combinations of nutrients for testing various relationships and finding the best simulation, but every index

indicates that the best model is **T°_NO_3_BFC_PO_4_PFC_LIGHT_SATURATION** *(Table 3)*:

	N°Parameters	RSS	E	AIC
T°_NO_3_BFC_PO_3_X_NO_3_PFC_LIGHT	10	0.774	0.381	-113.392
T°_NO_3_BFC_PO_4_NO_3_liebig_PFC_LIGHT	10	0.695	0.445	-117.183
T°_NO_3_BFC_PO_4_NO_3_arithmean_PFC_LIGHT	10	0.761	0.392	-114.002
T°_NO_3_BFC_PO_4_NO_3_harmonmean_PFC_LIGHT	10	0.763	0.39	-113.911
T°_NO_3_BFC_PO_4_X_$SiOH_4$_PFC_LIGHT	10	0.717	0.426	-116.064
T°_NO_3_BFC_PO_4_$SiOH_4$_liebig_PFC_LIGHT	10	0.73	0.416	-115.43
T°_NO_3_BFC_PO_4_$SiOH_4$_arithmean_PFC_LIGHT	10	0.716	0.427	-116.065
T°_NO_3_BFC_PO_4_SiOH4_harmonmean_PFC_LIGHT	10	0.717	0.427	-116.075

Table 4

T°_NO_3_BFC_PO_3_X_NO_3_PFC_LIGHT: in this model, before the Fish Farm closure NO_3 was inserted as limiting nutrient and after closure PO_4 and NO_3 were added as limiting nutrients; the value for the nutrients function were multiplied at each time.

T°_NO_3_BFC_PO_4_X_$SiOH_4$_PFC_LIGHT: in this model, before the Fish Farm closure NO_3 was inserted as a limiting nutrient followed by PO_4 and $SiOH_4$; the value for the nutrient function were multiplied at each time.

In the other model in *Table 4* "liebig" indicates that the nutrient was chosen by the *minimum of Liebig*, "arithmean" indicates that there is an arithmetic mean between the two nutrients:

$$f_{3b}(N) = \frac{N_1}{2 \cdot (k_{N1} + N_1)} + \frac{N_2}{2 \cdot (k_{N2} + N_2)} \quad (15)$$

$f_{3b}(N)$ is a variation of the equation (8); in this function N_1 is the concentration of the first nutrient, N_2 is the concentration of the second nutrient, k_{N1} is the semi-saturation constant of the first nutrient and k_{N2} is the semi-saturation constant of the second nutrient. "Harmonmean" indicates that there is a harmonic mean between both nutrients:

$$f_{3c}(N) = \frac{2}{N_1 \cdot (k_{N1} + N_1)} + \frac{2}{N_2 \cdot (k_{N2} + N_2)} \quad (16)$$

$f_{3c}(N)$ is a variation of the equation (8), where N_1 and N_2 are the concentration of the first and second nutrient, k_{N1} and k_{N2} are the semi-saturation constant of the first nutrient and the second nutrient.

BEST FISH FARM STATION MODELS

	N°Parameters	RSS	E	AIC
T°_NO_3_kvar_LIGHT_SATURATION	9	0.706	0.435	-118.62
T°_NO_3_BFC_PO_4_PFC_LIGHT_ SATURATION	9	0.693	0.446	-119.29
T°_NO_3_BFC_$SiOH_4$_PFC_LIGHT_ SATURATION	9	0.725	0.42	-117.698
T°_NO_3_BFC_PO_4_NO_3_liebig_PFC_LIGHT_SATURATION	10	0.695	0.445	-117.183

Table 5

Table 5 shows the best *Fish Farm Station* models, based on the results of the RSS, E and AIC indexes. The index results are similar, the best result was achieved by model **T°_NO_3_BFC_PO_4_PFC_LIGHT_ SATURATION.** Before the Fish Farm closure the conditions that regulated the *chlorophyll a* dynamics were the same in all the models in *Table 5*: temperature function (3), the nutrient that regulates the phytoplankton dynamics before the Fish Farm closure NO_3 with equation (8) and the light function with equation (5). All the models in *Table 5* include a change in the nutrient/s that regulate the phytoplankton dynamics after the Fish Farm closure: either in the k_N constant, or in the nutrient/s or both.

In conclusion, in all models the conditions before the Fish Farm closure are the same, the models differ only for the nutrients function (8) that changes after the Fish Farm closure.

FISH FARM MODEL VALIDATION

The validation consists of testing the best model of the *Fish Farm Station* with an independent set of data, in this specific case the *Station A* dataset. *Table 6* shows the result of validation of the best *Fish Farm Station* models (*Table 5*). For every four models in *Table 6* the index values resulting from the simulation after the calibration of the same models are also shown.

	N°Parameters	RSS	E	AIC
VALIDATION T°_NO_3_kvar_LIGHT_SATURATION	9	2.554	-2.06	-73.617
CALIBRATION T°_NO_3_kvar_LIGHT_SATURATION	9	2.158	-1.586	-79.511
VALIDATION T°_NO_3_BFC_PO_4_PFC_LIGHT_ SATURATION	9	2.658	-2.184	-72.228
CALIBRATION T°_NO_3_BFC_PO_4_PFC_LIGHT_ SATURATION	9	2.359	-1.827	-76.397
VALIDATION T°_NO_3_BFC_$SiOH_4$_PFC_LIGHT_ SATURATION	9	2.549	-2.054	-73.685
CALIBRATION T°_NO_3_BFC_$SiOH_4$_PFC_LIGHT_ SATURATION	9	2.278	-1.73	-77.61
VALIDATION T°_NO_3_BFC_PO_4_NO_3_liebig_PFC_LIGHT_SATURATION	10	2.559	-2.066	-71.547
CALIBRATION T°_NO_3_BFC_PO_4_NO_3_liebig_PFC_LIGHT_SATURATION	10	2.264	-1.712	-75.839

Table 6

In all the examples the index value for the validation is poor; this is evident from the results of RSS, E and AIC indices. The same models with the calibration also gives poor index results.

The table below shows only the simulation of two models of *Table 6* (one validation and one calibration); this is because all simulations are not good and similar. Therefore is not useful to see all the simulations of the model reported in *Table 6*.

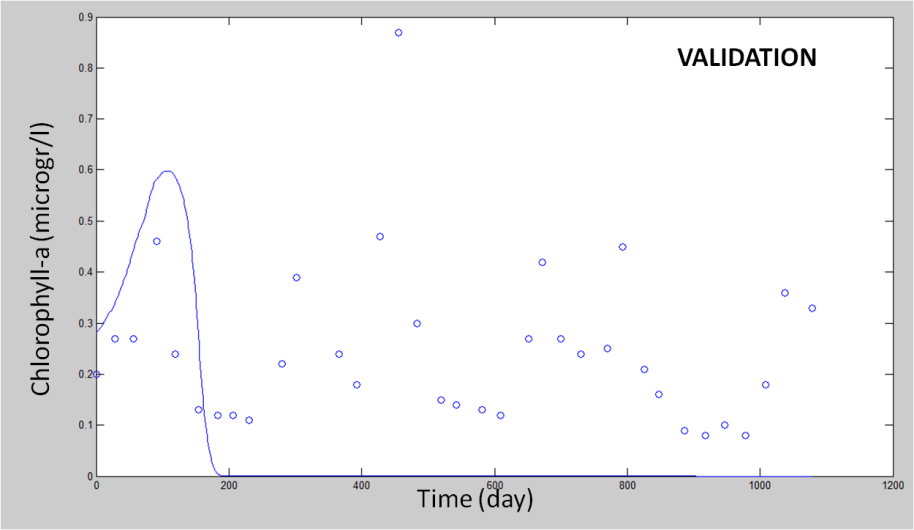

Simulation Graph 13

Simulation Graph 13 shows the validation of model **T°_NO_3_BFC_PO_4_PFC_LIGHT_SATURATION**: the Station A dataset was inserted in the *Fish Farm Station* model. The results of index (RSS, E and AIC) are

not good and the simulation data do not reflect the real pattern of *chlorophyll a*.

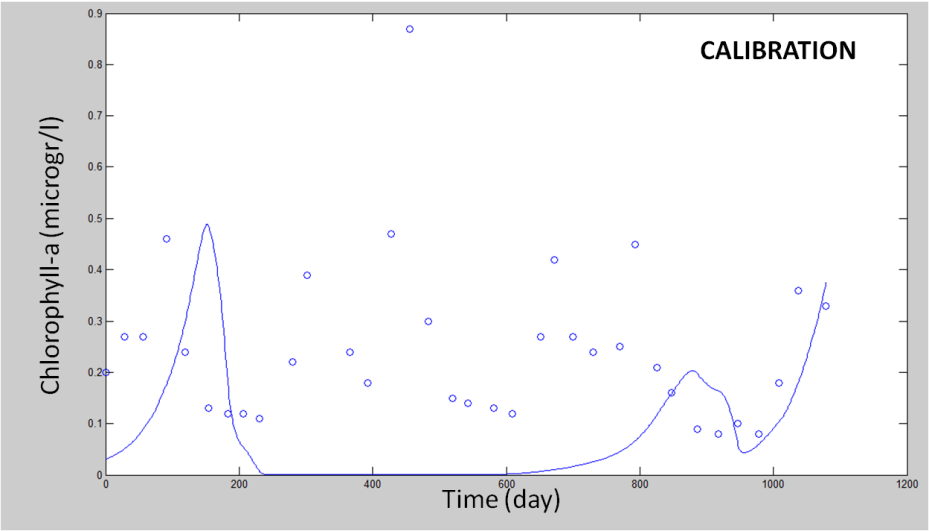

Simulation Graph 14

Simulation Graph 14 shows the preview model but with the calibration of all the parameters, this is the best result achieved.

SIMULATION OF *STATION A* MODELS

	N°Parameters	RSS	E	AIC
T°_NO_3_PO_4_SEASON_LIGHT_SATURATION	9	0.798	0.043	-114.314
T°_NO_3_PO_4_SEASON_LIGHT_SEASON_SATURATION	10	0.793	0.050	-112.575
T°_NO_3_PO_4_SEASON_LIGHT_SATURATION_kvar	11	0.329	0.606	-141.390
T°_NO_3_PO_4_SEASON_LIGHT_SEASON_SATURATION_kvar	12	0.327	0.608	-139.569

Table 7

To obtain a good simulation for *Station A* models that include a simplification for the seasonality of phytoplankton dynamics were made, in addition to the temperature function (3) and the light function (5). In all the models reported in *Table 7* it was decided that in winter and spring each year the nutrient to regulate *chlorophyll a* dynamics should be NO_3, which regulates the dynamics of *Cryptophyta* and *Chlorophyta* (more abundant in this season), whereas in summer and fall it should be PO_4 which regulates *Prochlorococcus* and *Synechococcus* dynamics, which are more abundant in this season (Al-Najjar et al. 2007, Mackey et al. 2007, Mackey et al. 2009). The previously explained seasonality of phytoplankton was not recreated directly by the model because it would double the number of parameters.

This would lead to a much too complex model (with many parameters), especially considering the few real *chlorophyll a* measurements. Therefore, the phytoplankton seasonality pattern was "forced" by making k_N change because there is a real change in the species that represented most of the *chlorophyll a*. In the Gulf of Aqaba, during *Prochlorococcus* and *Synechococcus* growth, some studies show that this Cyanobacteria have higher phosphorus than nitrogen requirements (Fuller et al. 2005, Mackey et al. 2009). The abbreviation "kvar" indicates that k_N can change after the *Fish Farm Station* closure.

The second and last models of *Table 7* show how if the simulation takes into account seasonality for the light function (with a k_L change of the light function, as for the nutrients) E improves slightly with respect to the models without seasonality for the light function, but AIC worsens.

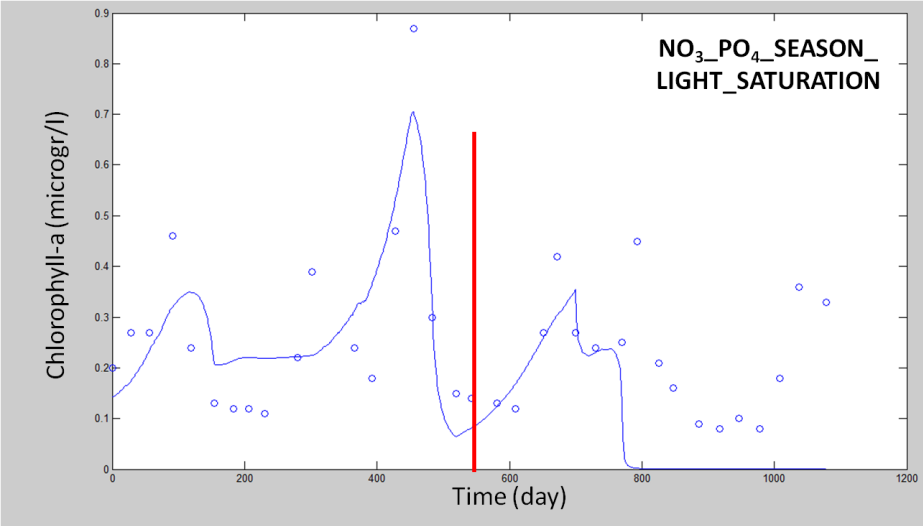

Simulation Graph 15

Simulation Graph 15 shows how after the Fish Farm closure the simulation was not good.

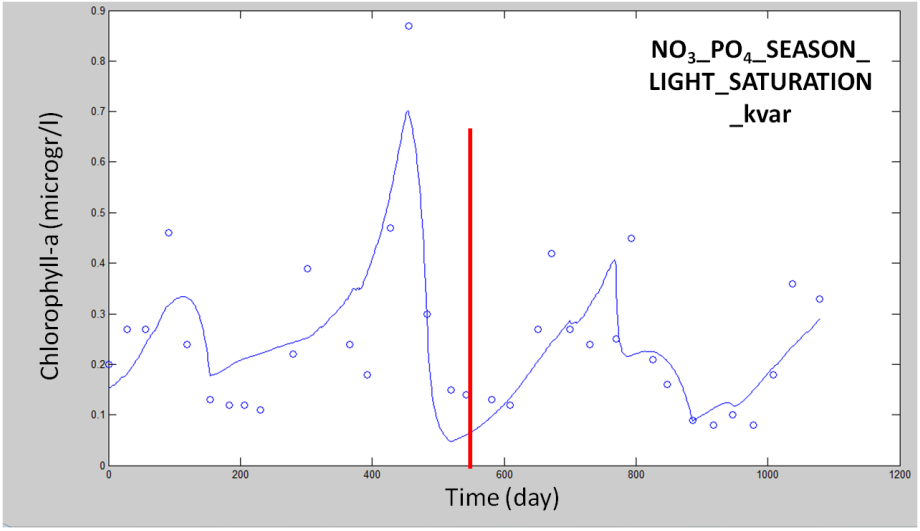

Simulation Graph 16

If the model includes the possibility for k_N to change after the Fish Farm closure, the model simulation and the index value improve, in particular after the red line (see *Simulation Graph 15*).

Models containing seasonality, with or without k_N being able to change after the *Fish Farm* closure, were applied to the *Fish Farm Station* dataset. *Table 8* shows the index values:

	N°Parameters	RSS	E	AIC
T°_NO_3_PO_4_SEASON_LIGHT_SATURATION	9	3.886498	-2.1074	-58.9244
T°_NO_3_PO_4_SEASON_LIGHT_SATURATION_kvar	11	3.732054	-1.98392	-56.3436

Table 8

In both models calibration was performed, but as seen by the index values, the element that controls the *Fish Farm Station* phytoplankton dynamics is the Fish Farm activity (*Table 5*) and not the seasonality (*Table 8*).

DISCUSSION

TIME SERIES

All the graphs of the time series after the Fish Farm closure, in particular the one about the *Fish Farm Station* data, show a decrease in the principal nutrients: NO_3, PO_4 and $SiOH_4$ (Fig. 9, Fig. 10 and Fig. 11). Thus, from 17th June 2008 onwards, when the Fish Farm closed, there is a lower concentration of nutrients. The *Fish Farm Station* nutrient concentration data are higher than those of *Station A*, but only before 17th June 2008, which was the date of the Fish Farm closure (Fig. 9, Fig. 10 and Fig. 11). This is the first statistically significant proof of the impact of the Fish Farm activities on at least the northernmost part of the Gulf, also hinting at a lesser effect on the entire Gulf as seen from the changes in nutrient concentrations at *Station A* before and after closure of the farming activity.

The graph of *chlorophyll a* reveals marked differences between *Fish Farm Station* data and *Station A* data. In particular, the *chlorophyll a* concentration is higher in the *Fish Farm Station* than it is in *Station A*; this is because there is a corresponding high nutrient concentration caused by the Fish Farm activity. This mean difference was greater (and statistically significant) before the fish farm closure (Huang et al. 2011). In both sampling stations the *chlorophyll a* concentration decreases over the sampling time (Fig. 8). In particular, lower *chlorophyll a* concentrations in both sampling stations are evident after the Fish Farm closure. This is more evident in the *Fish Farm Station* data (Fig. 8), but there is also a (weaker) decrease in *Station A* data. This might mean that the Fish Farm activity influences the concentration of nutrients which in turn influences the phytoplankton dynamics. This happens in both stations, but more markedly in the *Fish Farm Station* due to its proximity to the Fish Farm and its nutrient emissions. The model clearly underscores the validity of *chlorophyll a* and of phytoplankton as signal amplifiers for eutrophication processes and as such early warning management tools for marine conservation and management.

It is interesting to see how in *Station A* there are similar *chlorophyll a* concentration patterns during summer and winter months (in all the sampling years) (Fig. 7). This can be linked to the typical seasonal dynamics of phytoplankton in the gulf: when the nutrients and *chlorophyll a* concentration is high, in winter, eukaryotic algae in particular *cryptophyta* and *chlorophyta* dominate the phytoplankton community (Al-Najjar et al. 2007, Mackey et al. 2007, Mackey et al. 2009). When the nutrients and *chlorophyll a* concentration is low, in summer and fall, picophytoplankton, in particular *Prochlorococcus* and *Synechococcus* are more abundant with respect to other phytoplankton species (Al-Najjar et al. 2007, Mackey et al. 2007, Mackey et al. 2009). The same interpretation is not true for the *Fish Farm Station,* in particular before the Fish Farm closure (Fig. 7). The difference in the response of phytoplankton near the farms to seasonal nutrient inputs due to mixing from that of the open water pelagic domain is a text book example. It tells apart the exquisite sensitivity of oligotrophic phytoplankton assemblages, exemplified by *Station A*, to even minor eutrophication, from the insensitivity of nutrient replete ones to increase in nutrient availability.

The negative correlation of water temperature and *chlorophyll a* means that in the summer month, with an high value of irradiance, there are low *chlorophyll a* concentration while in winter, with a low value of irradiance, an high concentration of *chlorophyll a* (Fig. 6, Fig.8), that corresponds to the general phytoplankton dynamics in the Gulf of Aqaba (Al-Najjar et al. 2007, Mackey et al. 2007, Mackey et al. 2009). The lack of the typical pattern (high *chlorophyll a* concentration in winter months and low concentration in summer months) in the *chlorophyll a* time series probably indicates that there is a different process than temperature/light (that have a cyclical pattern: high value in summer months and low in winter) that regulates the phytoplankton dynamics, probably the nutrients. This is evident in the *Fish Farm Station* data, in particular in the summer and fall months, before the Fish Farm closure where is not possible to see the typical seasonality, instead the seasonality becomes more visible after

the Fish Farm closure and in all the three year *Station A chlorophyll a* data (Fig. 7).

In the graphs of NO_3 (Fig. 10) it is possible to see the peak in correspondence of the 15^{th} month (middle of march 2008), which was probably due to an event of upwelling caused by very intense deep mixing (Iluz et al. 2009). There is also the same situation for the PO_4 data, and the result of this nutrients increase is a strong spring bloom (Gordon et al. 1994, Genin et al. 1995). This is evident in the *chlorophyll a* time series for both the sampling stations: following high levels of this two nutrients there is an increase of the *chlorophyll a* concentration on months 15 and 16 (thus, a slightly time shifted effect), because PO_4 (in particular) and NO_3 are the main two nutrients limiting the phytoplankton growth rates in the Gulf of Aqaba (Suggett et al. 2009). From the correlations between *chlorophyll a* and these two nutrients it is evident how high concentrations of nutrients lead to corresponding high *chlorophyll a* concentrations, which is to be expected in a oligotrophic system such as the Gulf of Aqaba, especially underscored in the summer.

It is interesting to examine the dynamics of the $SiOH_4$: before the Fish Farm closure there is a particular time trajectory, with a fluctuating concentration of $SiOH_4$. After two months of the Fish Farm closure the trend became constant and very similar in both sampling stations. It is plausible that the *diatoms*, that are characterized by a unique cell wall made of silica, are implicated in this pattern, but since there are not cell count data available, it is not possible to confirm this hypothesis.

FISH FARM STATION MODELS

In the *Table 1* is evident how in all the models the *Arrhenius* exponential function is better than the *Optimum* function (RSS, E and AIC indices). This because the exponential model simulates the overall dynamics of all the phytoplankton species, like a sum of *chlorophyll a* concentration. Different phytoplankton species have different growth temperature optima and the *Arrhenius* function can be considered as a sum of optimum functions (Bowie et al. 1985). NO_3 and PO_4 explain better the real trend of

chlorophyll a than the $SiOH_4$ (*Table 1*): this is in agreement with the typical phytoplankton dynamics and limiting nutrients described in the Gulf of Aqaba (Al-Najjar et al. 2007, Mackey et al. 2007, Mackey et al. 2009, Suggett et al. 2009). In the models **T°(EXP)_NO_3** (*Simulation Graph. 2*) and **T°(EXP)_PO_4** (*Simulation Graph. 3*) the *chlorophyll a* concentration approaches to zero at the end of simulations because this two nutrients decrease over time (Fig. 9 and Fig. 10). In the function (8), if the nutrient concentration (N) decrease during the three years and the semisaturation constant (k_N) remains the same value, the results that chlorophyll approaches the zero value. The decrease of the nutrients is due to the closure of the Fish Farm, that during its activity caused an increase of nutrients concentration (Huang et al. 2011).

In the first three models of the *Table 2* phytoplankton dynamics were simulated with some combination of nutrients and a semisaturation constant that cannot change after the Fish Farm closure (equation (14) and minimum of Liebig), but with not good index results (RSS, E and AIC indices). In these models the Fish Farm impact is not explicitly simulated with a change of parameters. For example in the model **T°_PO_4_X_NO_3** the phytoplankton dynamics is driven by the interaction between the PO_4 and NO_3 within equation (14). The results of this simulation as represented by indices of performance are not very good.

In the Gulf of Aqaba the typical seasonal dynamics shows that when the nutrient concentrations are very low, in particular in summer and fall, *Prochlorococcus* and *Synechococcus* represent a significant portion of the phytoplankton community and some studies show that these taxa have higher phosphorous requirements relative to nitrogen (Al-Najjar et al. 2007, Mackey et al. 2007, Mackey et al. 2009), which is not surprising in the light of reports of nitrogen fixin capabilities in some *Synechococcus* isolates (Agawin et al. 2007). During winter and spring, when there is a deeply mixed water body, and nutrient level increase, *Cryptophyta* and *Chlorophyta* account for most of the phytoplankton community, that is generally limited by light, but not in the upper euphotic zone, where, in this case, nitrogen explains the *chlorophyll a* dynamics (Mackey et al. 2009).

Therefore an increase in nutrient concentrations caused by natural activity, such as mixing, should cause a change in phytoplankton dynamics. Since the Fish Farm activity had caused an increase in nutrients concentration, it probably caused a consequent change in the phytoplankton dynamics (Takamura et al. 1992, Flander-Putrle and Malej 2003).

For this reason the semi-saturation constant changed after the Fish Farm closure (last six models of *Table 2*). Model **T°_NO_3_kvar** has a better index value with respect to model **T°_PO_4_kvar.** This might be due to the Fish Farm activity: normally the Gulf of Aqaba is limited mainly by phosphate, but with the Fish Farm activity the nutrient that better simulates the phytoplankton dynamics is nitrogen (Chen et al 2007). In particular, *Simulation Graph 5* and *Simulation Graph 6* show how before the red line NO_3 explains better the real trend of *chlorophyll a* than PO_4 does. In both simulation graphs the index value (RSS, E and AIC indices) are better than the previous models (*Table 1*) where the semi.-saturation constant (k_N) in the equation (8) remained the same over the three years, because there was a change in algal communities and the variation of the k_N value was able to simulate it. In *Simulation Graph 7* of model **T°_NO_3_BFC_PO_4_PFC** it was decided that the nutrient that regulates the phytoplankton dynamics before the Fish Farm closure, with higher concentration of nutrients, was nitrogen and after the Fish Farm closure, with a lower nutrient concentration, was phosphate; the index results confirm that is a correct interpretation of the Fish Farm activity (*Table 2*). Model **T°_NO_3_BFC_$SiOH_4$_PFC** gave similar index results (*Table 2*). That result, together with the index results of the **T°_NO_3_BFC_PO_4_PFC** and **T°_NO_3_kvar** models (*Table 2*), strongly suggest that before the Fish Farm closure nitrogen was the best nutrient to regulate phytoplankton dynamics. Before the Fish Farm closure, there was a high nutrient concentration caused by the Fish Farm activity, which might have led to similar phytoplankton dynamics to the normal winter phytoplankton dynamics (without Fish Farm): high nutrient concentration and *Cryptophyceae* and *Chlorophyceae* that make up most of the phytoplankton community. *Diatoms* might also be implicated in this pattern (Fig. 11), but there are no counting cell data available to support that. After the Fish Farm

closure it is interesting to see how the models which simulate a change in the nutrient limiting growth rate, in the form of nutrient change (*Simulation Graph 7 and Simulation Graph 8*) or semi-saturation constant change (*Simulation Graph 5*), better explain the real *chlorophyll a* pattern.

Table 3 shows models with the added light limiting function, with optimum function (*Steel formulation*) (7) and saturation function (*Michaelis-Menten*) (5). In all models the best function to simulate the phytoplankton dynamics is the saturation function; this is because the simulation involves a large set of phytoplankton species and there is no optimum value for all the species. In particular, *Simulation Graph 10* and *Simulation Graph 12* show how the optimum function for light causes major fluctuations; this is due to the presence of the optimum that causes a maximum growth for the phytoplankton dynamics at the optimum irradiance value. It is interesting to see how all index values for the models in *Table 3* improve (compared to *Table 2* and *Table 1*), if the light parameter is added to the function (5). That suggests that light has an important function in this ecosystem, and is essential to obtain a good simulation.

Table 4 shows models with different nutrient interaction, with equation (15), (16) and the *minimum of Liebig*. Compared to the most complex models of *Table 3* that contain 9 parameters, there are not large differences between the RSS and E index values, but the AIC index values are worse. Indeed the RSS and E indexes do not take into account the number of parameters and therefore no particular differences between the values of Table 3 and 4 were found. The models in *Table 4* have a higher number of parameters compared to the models in *Table 3*, which explains the worse AIC index values. Thus, if the models have the same or similar E and RSS index values, but a lower AIC index value, the simplest model with the lowest number of parameters is better.

Table 5 summarizes the best models with their index values from the *Fish Farm Station* models. All the best models in *Table 5* have two particular characteristics in common: each model includes a variation concerning the limiting nutrient after the Fish Farm closure, and, in particular, in all the models in *Table 5* only nitrogen regulates the

phytoplankton dynamics before the Fish Farm closure. This means that during the Fish Farm activity the phytoplankton dynamics, in the first meter of depth, was driven primarily by the nitrogen concentration. This is due to the Fish Farm impact that produced particular phytoplankton dynamics: the phytoplankton species abundance was roughly similar to that of a normal situation (without Fish Farm), but the abundance of the cell number per species was unbalanced. If few species accounted for most of the detected *chlorophyll a*, in the simulation of the total *chlorophyll a* concentration, the phytoplankton dynamics will be regulated only by the factors that limit the growth of a few species representing most of total *chlorophyll a* concentration. In fact, the only way to get a good simulation before the Fish Farm closure was to put nitrogen in the models as the only limiting nutrient. Probably, during the Fish Farm activity, the species that represented most of the phytoplankton community were those that are typically present in the Gulf of Aqaba during winter and spring, with a high nutrient concentration (*Cryptophyceae* and *Chlorophyceae*). During the Fish farm activity *Prochlorococcus* and *Synechococcus* were probably scarcely present, since they represent, in an amount of *chlorophyll a*, the majority of the phytoplankton community in summer and fall with a low nutrient concentration (Al-Najjar et al. 2007, Mackey et al. 2007, Mackey et al. 2009). Furthermore, the growth of *Prochlorococcus* and *Synechococcus* is generally driven by phosphate (Fuller et al. 2005, Mackey et al. 2009), and all the best models before the Fish Farm closure were influenced by nitrogen (*Table 5*). After the Fish Farm closure different nutrient combinations gave similar results and there is not a single solution which seems most plausible, see *Table 5* (RSS, E and AIC indices). Probably, after the Fish Farm closure the *chlorophyll a* concentration was distributed more evenly within the phytoplankton species present. In fact, after the Fish Farm closure different nutrient options led to similar results. The different nutrient effect (on the determination of phytoplankton dynamics) might also be approximately the same because, after the Fish Farm closure, there is a decrease in the concentrations of all the nutrients and *chlorophyll a*.

STATION A MODELS

Table 6 illustrates the validation and the calibration of the best models in *Table 5*. All the index values (RSS, E and AIC) are not good for the validation or for the calibration. The poor index values concerning validation and calibration mean that the best *Fish Farm Station* models (*Table 6*) are not valid for *Station A* data. The Fish Farm activity might have influenced *Fish Farm Station* sampling point data much more than the *Station A* sampling point. *Simulation Graph 13* and *Simulation Graph 14* show how the model with the best simulation for the *Fish Farm Station* data, does not give good results for *Station A* data, even after the calibration. The same results can be seen in the index values reported in *Table 6*. Those results indicate that the model that represents a good simulation for the *Fish Farm Station* data is unfit to define the phytoplankton dynamics for *Station A* data.Thus, it seems that in the *Station A* ecological system, the forces acting to determine the phytoplankton dynamics are different from those that act in the *Fish Farm Station*.

In *Table 7* the models were constructed by imposing the seasonality of the phytoplankton, to see if that improves the simulation and to understand what forces determinate the phytoplankton dynamics. In the first model in *Table 7* seasonality was inserted only for the limiting nutrient function, whereas in the second model, in addition, seasonality for the light function was inserted: the E index improves but the AIC index gets worse, indicating that unnecessary complexity was added. To build the models the solar year was divided into two parts: summer/fall and winter/spring, which correspond to mixing and no mixing periods. In the months that include summer/fall PO_4 was inserted as the limiting nutrient, which should regulate the growth of most of the phytoplankton community (*Prochlorococcus* and *Synechococcus*) in this part of the year (Al-Najjar et al. 2007, Mackey et al. 2007, Mackey et al. 2009). In the months that include winter/spring NO_3 inserted as the limiting nutrient, which should regulate the growth of *Cryptophyta* and *Chlorophyta* being more abundant in winter and with higher nutrient concentrations (Al-Najjar et al. 2007, Mackey et al. 2007, Mackey et al. 2009). Therefore, by inserting in the model the seasonality for

the phytoplankton community, a good simulation of the total *chlorophyll a* was achieved; however the index values were still not good, because the simulation approaches zero around day 800 (*Table 7* and *Simulation Graph 15)*. A better simulation was obtained in the last two models in *Table 7*: the same preview models are shown, but with a difference; the semi-saturation constant (k_N) for the nutrient function can change after the Fish Farm closure. In this case the index value greatly improves with respect to the first two models in *Table 7*. When comparing *Table 6* with *Table 7* the Fish Farm impact appears to be much lower than the impact in the *Fish Farm Station* (*Table 5*); this is because the phytoplankton dynamics appears to be driven mainly by the seasonal mixing cycle. It was chosen to "force" the seasonal succession of the algal community on the models in *Table 7*, whereas it was not possible to make it "emerge" directly from the model by simulating explicitly the two different algal groups, because this would have required a doubling of the parameters in the model. This would have created too complex a model for the few fitting data available. In addition, precise information on the parameter values regarding the two algal groups are lacking, and this would have complicated the fitting (indeed a tentative fitting was tried for such a 2-population model, although it is not reported, and it did not work properly).

In conclusion, the best results for *Station A* indicate that the principal forces that determinate the phytoplankton dynamics in that station are the mixing, and as a consequence the nutrient concentration, which determine the seasonal succession in the algal community, and also the Fish Farm activity.

CONCLUSIONS

The statistical analysis on the *Fish Farm Station* dataset shows that there are significant differences within the sampling station (high value of *chlorophyll a* and nutrients before the Fish Farm closure and low concentration after it). This demonstrates that the Fish Farm activity had altered the nutrient concentrations and as a consequence the normal phytoplankton dynamics. This finding was confirmed by model simulations. In particular, thanks to the simulations, it was possible to understand that during the Fish Farm activity it was nitrogen that influenced phytoplankton dynamics throughout the year, whereas after the closure there were various combinations of nutrients which explain the phytoplankton dynamics. This finding is particularly important because it suggests that during the Fish Farm activity the number of individuals within the species that made up the measure of total *chlorophyll a* were probably unbalanced (many individuals for few species and few individuals for many species), which is consistent with the commonly-held interpretation of eutrophication, which is expected to reduce community diversity (Cottingham and Carpenter 1998, Pitta et al. 1998), with fast responding "r" strategist, opportunistic species becoming rapidly dominant. After the Fish Farm closure the number of individuals within species is probably distributed more evenly among more species. In either case this is explained by the models in *Table 5*: different limiting nutrients can be introduced, with similar results. So the Fish Farm activity in the model assumes more importance than the natural sequence of events that normally drives the seasonal phytoplankton patterns in the Gulf of Aqaba. Here we have a clear case of physics driving chemistry, leading to biological response, a sequence perturbed by human intervention. The Fish Farm impact is so strong that the best models for the Fish Farm do not need to take into account seasonality to get good results (Tab. 8). After the Fish Farm closure there is a gradual return to normal physics driven conditions; unfortunately it was not possible to test the reestablishment of seasonality dominance after the Fish Farm closure on the *Fish Farm Station* dataset because there were insufficient data.

The statistical analysis for the *chlorophyll a* concerning *Station A* shows that before and after the Fish Farm closure there are no significant differences. This might mean that there was little impact on *Station A* by the Fish Farm activity. However, the statistical analysis does show a significant difference in nutrients, which decreased after the Fish Farm closure. Thus, in the *Station A* models, to obtain a good simulation, it is essential to incorporate seasonality but, also, it is important to consider a Fish Farm impact that improves all the index values (RSS, E and AIC) (*Table 7*). Despite the distance between the two sampling stations (about 13 km), there might be an influence from the Fish Farm activities also on the *Station A* ecosystem, which altered the normal phytoplankton dynamics patterns. To fully understand this the annual nitrogen and phosphorus outputs of the 3000 tonns of fish at peak volume, have to be diluted by the entire volume of the Gulf, taking into account also the rather limited water exchange with the Red Sea. This impact appears to be much lower than the impact next to the *Fish Farm Station*, because the open- sea phytoplankton dynamics in the pelagic domain appears to remain driven mainly by the seasonal mixing cycle, as shown by the comparison of *Table 6* with *Table 7*.

The statistical analysis carried out between *Station A* and the *Fish Farm Station* shows significant differences before the Fish Farm closure. Conversely, after the closure there were no significant differences. This might mean that the forces that determine the phytoplankton dynamics are different in the two sampling stations during the period when the fish farm was open. From the statistical analysis it is not possible to identify what those differences are; instead, these differences are highlighted in the results obtained from model simulations, highlighting the importance of ecological modelling in providing better understanding of the functioning of the Gulf of Aqaba ecosystem. Subsequent work requires the development of compatible models of the Gulf's benthic domains, dominated by its coral reefs, and ultimately a merging of both models revealing energy and material fluxes between sea and reef.

REFERENCES

Agawin NSR, Rabouille S, Veldhuis MJW, Servatius L, Hol S, Van Overzee HMJ, Huisman J (2007): Competition and facilitation between unicellular nitrogen-fixing cyanobacteria and non-nitrogen-fixing phytoplankton species. Limnology and Oceanography, 52: 2233-2248

Akaike H (1974): A new look at the statistical model identification. IEEE Transactions on Automatic Control, 19: 716–723

Al-Najjar T, Badran MI, Richter C, Meyerhoefer M, Sommer U (2007): Seasonal dynamics of phytoplankton in the Gulf of Aqaba, Red Sea. Hydrobiologia, 579: 69-83

Al-Qutob M, Häse C, Tilzer MM, Lazar B (2002): Phytoplankton drives nitrite dynamics in the Gulf of Aqaba, Red Sea. Marine Ecology Progress Series, 239: 233-239

Bowie GL, Mills WB, Porcella DB, Campbell CL, Pagenkopf JR, Rupp GL, Johnson KM, Chan PWH, Gherini SA (1985): Rates, constants, and kinetics formulations in surface water quality modeling. Second edition. Tetra Technology Report, No. EPA/600/3-85-040, pp 475.

Chen Y, Mills S, Street J, Golan D, Post A, Jacobson M, Paytan A (2007): Estimates of atmospheric dry deposition and associated input of nutrients to Gulf of Aqaba seawater. Journal of Geophysical Research, 112: D04309

Chen Y, Paytan A, Chase Z, Measures C, Beck AJ, Sanudo-Wilhelmy SA, Post A F (2008): Sources and fluxes of atmospheric trace elements to the Gulf of Aqaba, Red Sea. Journal of Geophysical Research, 113: D05306

Cottingham KL and Carpenter SR (1998): Population, community, and ecosystem variates as ecological indicators: Phytoplankton responses to whole-lake enrichment. Ecological Applications, 8: 508-530

Flander-Putrle V and Malej A (2003): The trophic state of coastal waters under the influence of anthropogenic sources of nutrients (fish farm, sewage outfalls). Periodicum Biologorum, 105(4): 359-365

Fuller NJ, West NJ, Marie D, Yallop M, Rivlin T, Post AF, Scanlan DJ (2005): Dynamics of community structure and phosphate status of picocyanobacterial populations in the Gulf of Aqaba, Red Sea. Limnology and Oceanography, 50: 363-375

Genin A, Lazar B, Brener S (1995): Vertical mixing and coral death in the Red Sea following the eruption of Mount Pinatubo. Nature, 377: 507-510

Gordon N, Angel DL, Neori A, Kress N, Kimor B (1994) Heterotrophic dinoflagellates with symbiotic cyanobacteria and nitrogen limitation in the Gulf of Aqaba. Marine Ecology Progress Series, 107: 83-88

Häse C, Al-Qutob M, Dubinsky Z, Ibrahim EA, Lazar B, Stambler N, Tilzer MM (2006): A system in balance? Implication in deep vertical mixing for the nitrogen budget in the northern Red Sea, including the Gulf of Aqaba (Eilat). Biogeosciences Discussions, 3: 383-408

Hill MN (1963): Global coastal ocean multiscale interdisciplinary processes. Volume 2: The composition of sea-water: comparative and descriptive oceanography. General Editor. Cambridge, Massachusetts and London. Pp 588

Huang YCA, Hsieh HJ, Huang SC, Meng PJ, Chen YS, Keshavmurthy S, Nozawa Y, Chen CA (2011):Nutrient enrichment caused by marine cage culture and its influence on subtropical coral communities in turbid waters. Marine Ecology Progress Series, 423: 83-93

Iluz D, Yehoshua Y, Dubinsky Z (2008): Quantum yields of phytoplankton photosynthesis in the Gulf of Aqaba (Elat), northern Red Sea. Israel Journal of Plant Sciences, 56: 29-36

Iluz D, Dishon G, Capuzzo E, Meeder E, Astoreca R, Montecino V, Znachor P, Ediger D, Marra J (2009): Short-term variability in primary productivity during a wind-driven diatom bloom in the Gulf of Eilat (Aqaba). Aquatic Microbial Ecology, 56: 205-215

Jørgensen SE and Bendoricchio G (2001): Foundamentals of ecological modelling. Third Edition. Elsevier. Oxford. Pp 530

Karl DM, BjöKrkman KM, Dore JE, Fujieki L, Hebel DV, Houlihan T, Letier RM, Tupas LM (2001): Ecological nitrogen-to-phosphorus stoichiometry at station ALOHA. Deep-Sea Research II, 48: 1529-1566

Labiosa RG, Arrigo KR, Genin A, Monismith SG, van Dijken G (2003): The interplay between upwelling and deep convective mixing in determining the seasonal phytoplankton dynamics in the Gulf of Aqaba: evidence from SeaWiFS and MODIS. Limnology and Oceanography, 48: 2355-2368

Lazar B, Erez J, Silverman J, Rivlin T, Rivlin A, Dray M, Meeder M, Iluz D (2008): Recent environmental changes in the chemical-biological oceanography of the Gulf of Aqaba (Eilat). In: Aqaba-Eilat, the Improbable Gulf. Environment, Biodiversity and Preservation (Editor: Por, F.D.). Magnes Press, Jerusalem: p. 49-62

Levanon-Spanier I, Padan E, Reiss Z (1979): Primary production in a desert-enclosed sea: the Gulf of Elat (Aqaba), Red Sea. Deep Sea Research I, 26: 673-686

Lindell D and Post AF (1995): Ultraphytoplankton succession is triggered by deep winter mixing in the Gulf of Aqaba (Eilat), Red Sea. Limnology and Oceanography, 40:1130-1141

Loya Y, Kramarsky-Winter E (2003): In situ eutrophication caused by fish farms in the northern Gulf of Eilat (Aqaba) is beneficial for its coral reefs: a critique. Marine Ecology Progress Series, 261: 299–303

Loya Y, Lubinevsky H, Rosenfeld M, Kramarsky-Winter E (2004): Nutrient enrichment caused by in situ fish farms at Eilat, Red Sea is detrimental to coral reproduction. Marine Pollution Bulletin, 49: 344-353

Mackey KRM, Labiosa RG, Calhoun M, Street JH, Post AF, Paytan A (2007): Phosphorus availability, phytoplankton community dynamics, and taxon-specific phosphorus status in the Gulf of Aqaba, Red Sea. Limnology and Oceanography, 52: 873-885

Mackey KRM, Rivlin T, Grossman AR, Post AF, Paytan A (2009): Picophytoplankton responses to changing nutrient and light regimes during a bloom. Marine Biology, 156: 1531-1546

Monismith SG, Genin A, Reidenbach MA, Yahel G, Koseff JR (2006): Thermally driven exchanges between a coral reef and the adjoining ocean. Journal of Physical Oceanography, 36: 1332-1347

Moriasi DN, Arnold JG, Van Liew MW, Bingner RL, Harmel RD, Veith TL (2007): Model evaluation guidelines for systematic quantification of

accuracy in watershed simulations. Transactions of the ASABE. Vol. 50: 885-900

Nash JE, Sutcliffe JV (1970): River flow forecasting through conceptual models part I — A discussion of principles. Journal of Hydrology, 10: 282-290

Paytan A, Mackey KRM, ChenY, Lima ID, Doney SC, Mahowald N, Labiosa R, Post AF (2009): Toxicity of atmospheric aerosol on marine phytoplankton. Proceedings of the National Academy of Science, 106: 4601-4605

Pitta P, Karakassis I, Tsapakis M, Zivanovic S (1998): Natural vs. mariculture induced variability in nutrients and plankton in the eastern Mediterranean. Hydrobiologia, 391: 181-194

Post AF, Veldhuis M, Lindell D (1996): Spatial and temporal distribution of ultraphytoplankton in the Gulf of Aqaba, Red Sea. Journal Phycology, 32: 38-39

Richter C, Wunsch M, Rasheed M, Kotter I, Badran MI (2001): Endoscopic exploration of the Red Sea coral reefs reveals dense populations of cavity-dwelling sponges. Nature, 413: 726-730

Stambler N (2005): Bio-optical properties of the northern Red Sea and th Gulf of Eilat (Aqaba). Journal of Sea Research, 54: 186-203

Stambler N (2006): Light and picophytoplankton in the Gulf of Eilat (Aqaba). Journal of Geophysical Research 111: C11009, doi:10.1029/2005JC003373

Suggett DJ, Stambler N, Prášil O, Kolber Z, Quigg A, Vázquez-Dominguez E, Zohary T, Berman T, Iluz D, Levitan O, Lawson T, Meeder E,

Lazar B, Bar-Zeev E, Medova H, Berman-Frank I (2009): Nitrogen and phosphorus limitation of oceanic microbial growth during spring in the Gulf of Aqaba. Aquatic Microbial Ecology, 56: 227-239

Sverdrup HU (1953): On conditions for the vernal blooming of phytoplankton. Journal du Conseil, 18: 287-295

Tagliabue A and Arrigo KR (2003): Anomalously low zooplankton abundance in the Ross Sea: an alternative explanation. Limnology and Ocenography, 48: 686-699

Takamura N, Zhu X, Yang H, Ye L, Hong F, Miura T (1992): High biomass and production of picoplankton in a Chinese integrated fish culture pond. Hydrobiologia, 237: 15-23

Wolf-Vetch A, Paldor N, Brenner S (1992): Hydrographic indications of advenction/convenction effects in the Gulf of Elat. Deep-Sea Research I, 39: 1393-1401

Yael G, Post AF, Fabricius K, Marie D, Vaulot D, Genin A (1998): Phytoplankton distribution and grazing near coral reefs. Limnology and Oceanography, 43: 551-563